River Dynamics Modeling

Weiming Wu, PhD
Professor
Dept. of Civil and Environmental Eng.
Clarkson University
Potsdam, NY 13699, USA

Updated on Oct. 9, 2014

Turbulence Closure

The often used turbulence closure models are based on Boussinesq's eddy viscosity concept:

$$\tau_{ij} = \rho \nu_t \left(\frac{\partial u_i}{\partial x_j} + \frac{\partial u_j}{\partial x_i} \right) - \frac{2}{3} k \delta_{ij}$$

- **Zero-equation turbulence models**
  - Mixing length model
  - Subgrid model

- **Two-equation turbulence models**
  - Standard k-ε turbulence model
  - RNG k-ε turbulence model
  - Nonequilibrium k-ε turbulence model
  - k-ω turbulence model

- **Other advanced models**: Non-linear k-ε turbulence model, Reynolds stress/flux model, algebraic Reynolds stress/flux model, LES, DNS, etc.

Movable Bed Roughness Formula

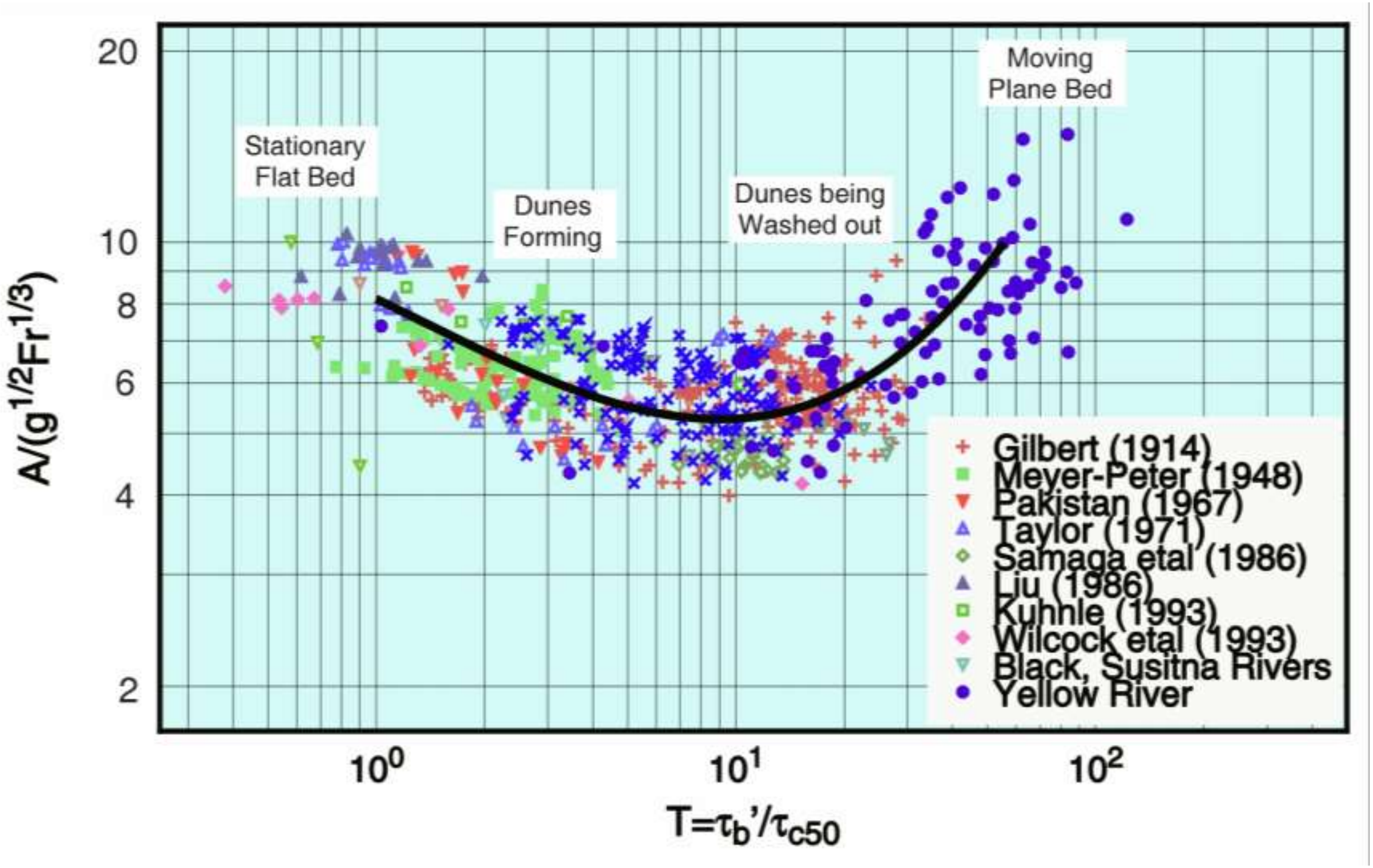

Wu and Wang (1999, JHE)

Comments on Manning's *n*

The existing movable bed roughness formulas are applicable only in cases with sediment grains, ripples and dunes.

In general, there are other contributors to the channel roughness, including channel training works, hydraulic structures, vegetation, alternate bars, islands, channel curvature, and alignment.

The most reliable approach to handling the channel roughness is still calibration using the available data measured at the study site.

In the cases where the banks and bed have different roughness features or floodplains exist, composite Manning's n or conveyance should be used.

Good references for Manning's n: Chow (1959), Fasken (1963), Barnes (1967), and Hicks and Mason (1991). USGS web site http://wwwrcamnl.wr.usgs.gov/sws/fieldmethods/Indirects/nvalues/index.htm

Sediment Adaptation Length

- For Bed Load
  - L_b: Related to the scales of dominant bed forms and channel geometry

- For Suspended Load

$$L_s = Uh / \alpha \omega_{sk}$$

  - α: Determined by empirical formula such as Armanini and di Silvio's (1988) method; or given 0.25-1.0.

- For Bed Material Load
  - $L = \max(L_b, L_s)$

Lags between Flow and Sediment

- Lag between local flow and sediment velocities
  - Considered in two-phase flow models, but usually ignored in most models available.
- Depth-averaged velocity difference
  - Considered
- Sediment deposition and erosion at the bed
  - Considered
- Bed form development, etc.
  - Less known and need to be investigated.

Ratio of Depth-Av. Sediment and Flow Velocities

$$\beta_s = \int_a^h u_s c dz \Big/ \left(U_c \int c dz \right)$$

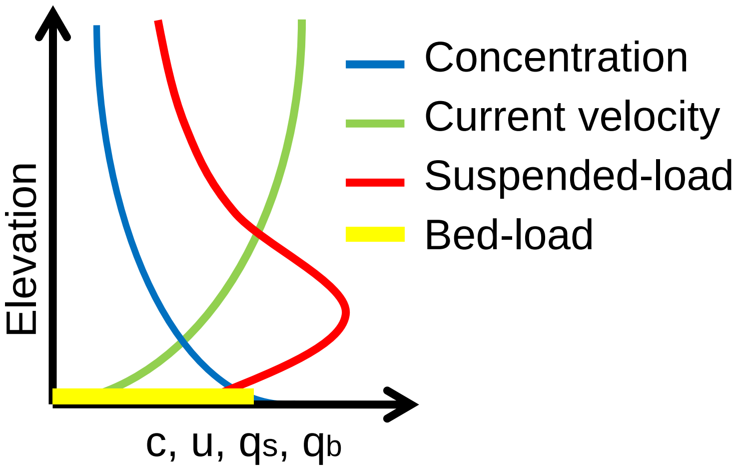

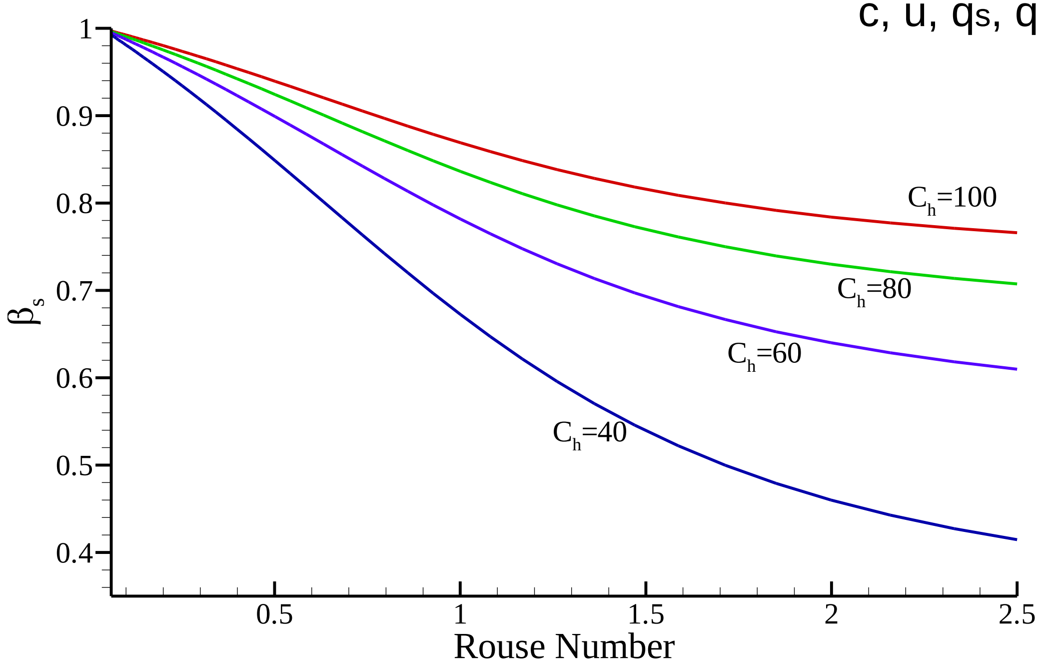

Modified van Rijn’s (1984) formula

$$\frac{u_b}{\sqrt{(\gamma_s/\gamma - 1)gd}} = 1.64T^{0.5}$$

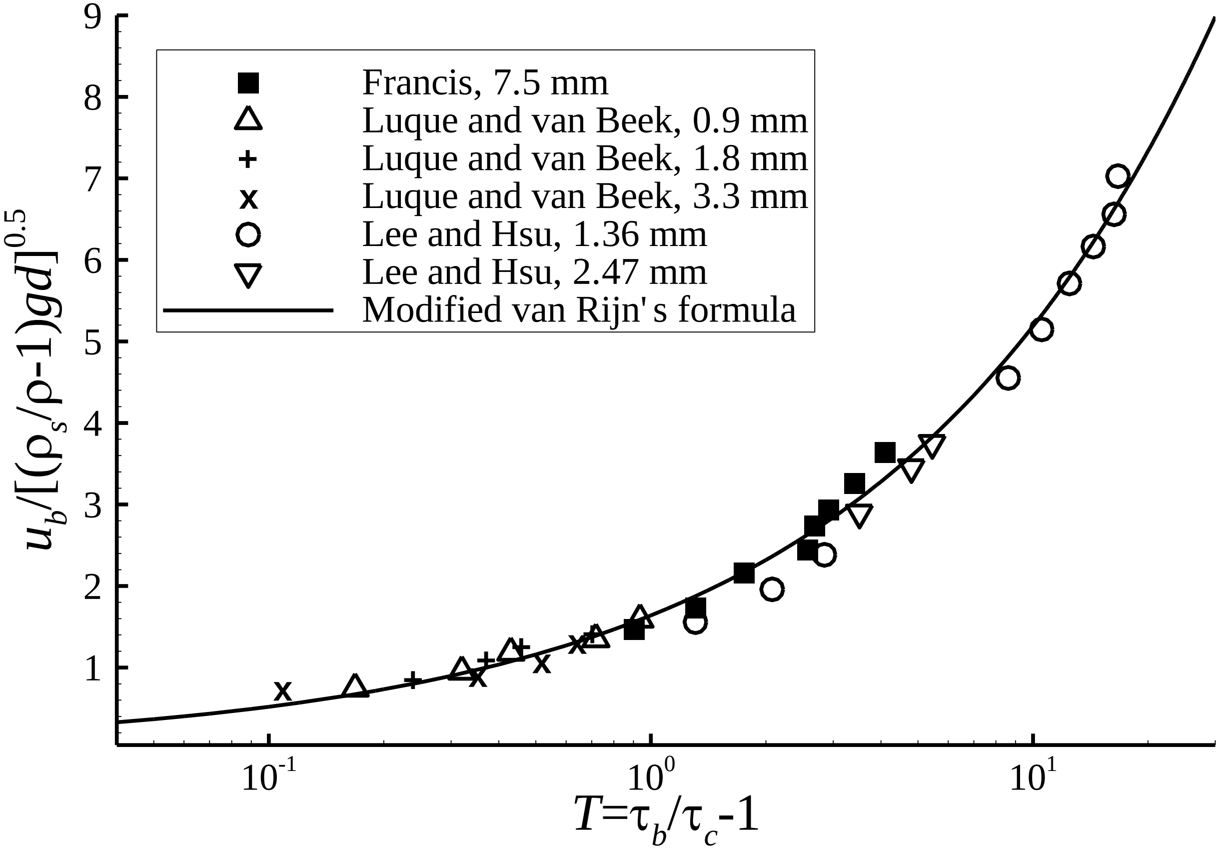

Wu et al. (2000) Bed Load Formula

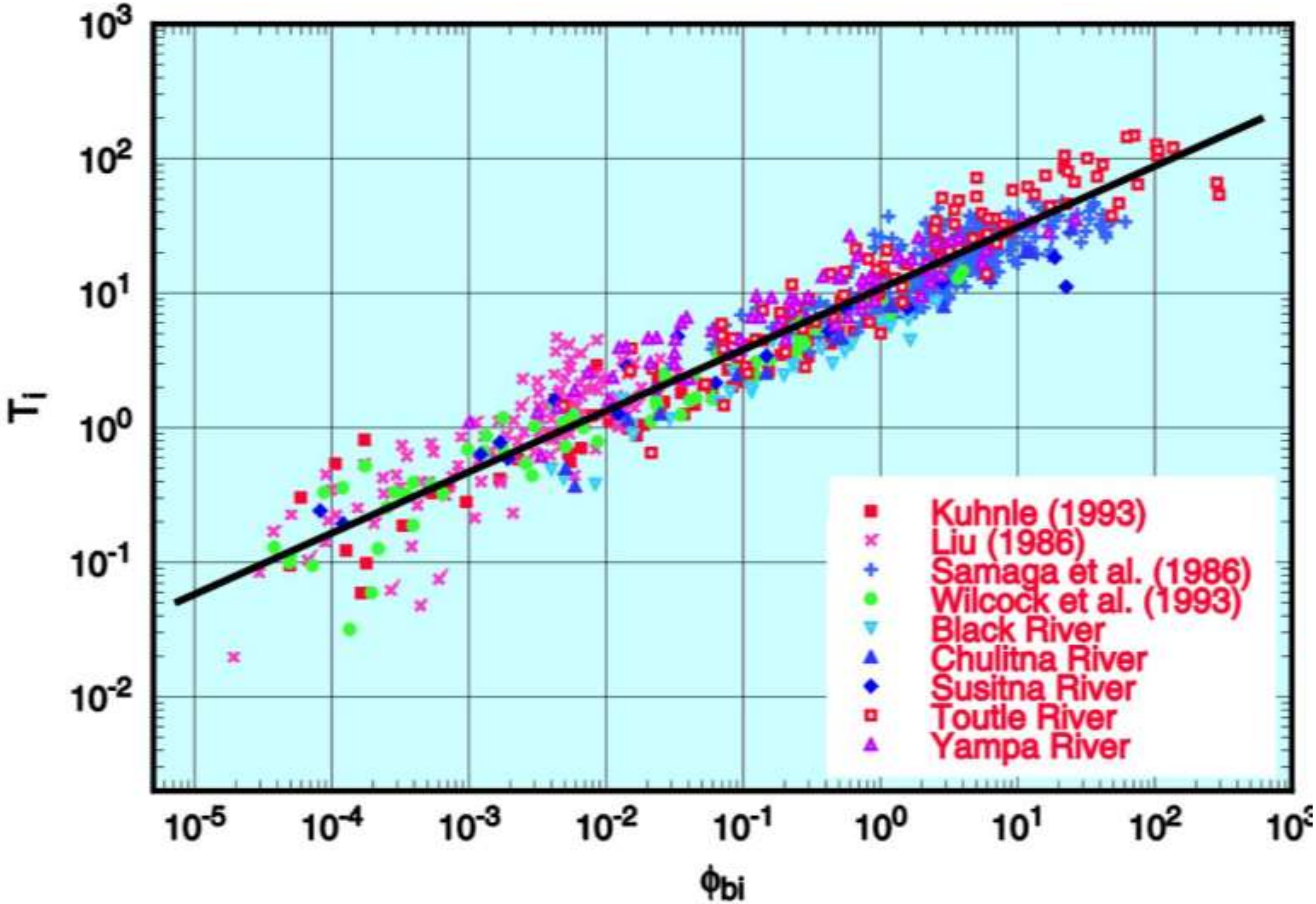

$$\frac{q_{bk}}{p_{bk}\sqrt{\left(\gamma_s/\gamma-1\right)gd_k^3}}=0.0053\left[\left(\frac{n'}{n}\right)^{3/2}\frac{\tau_b}{\tau_{ck}}-1\right]^{2.2}$$

Wu et al. (2000) Suspended Load Formula

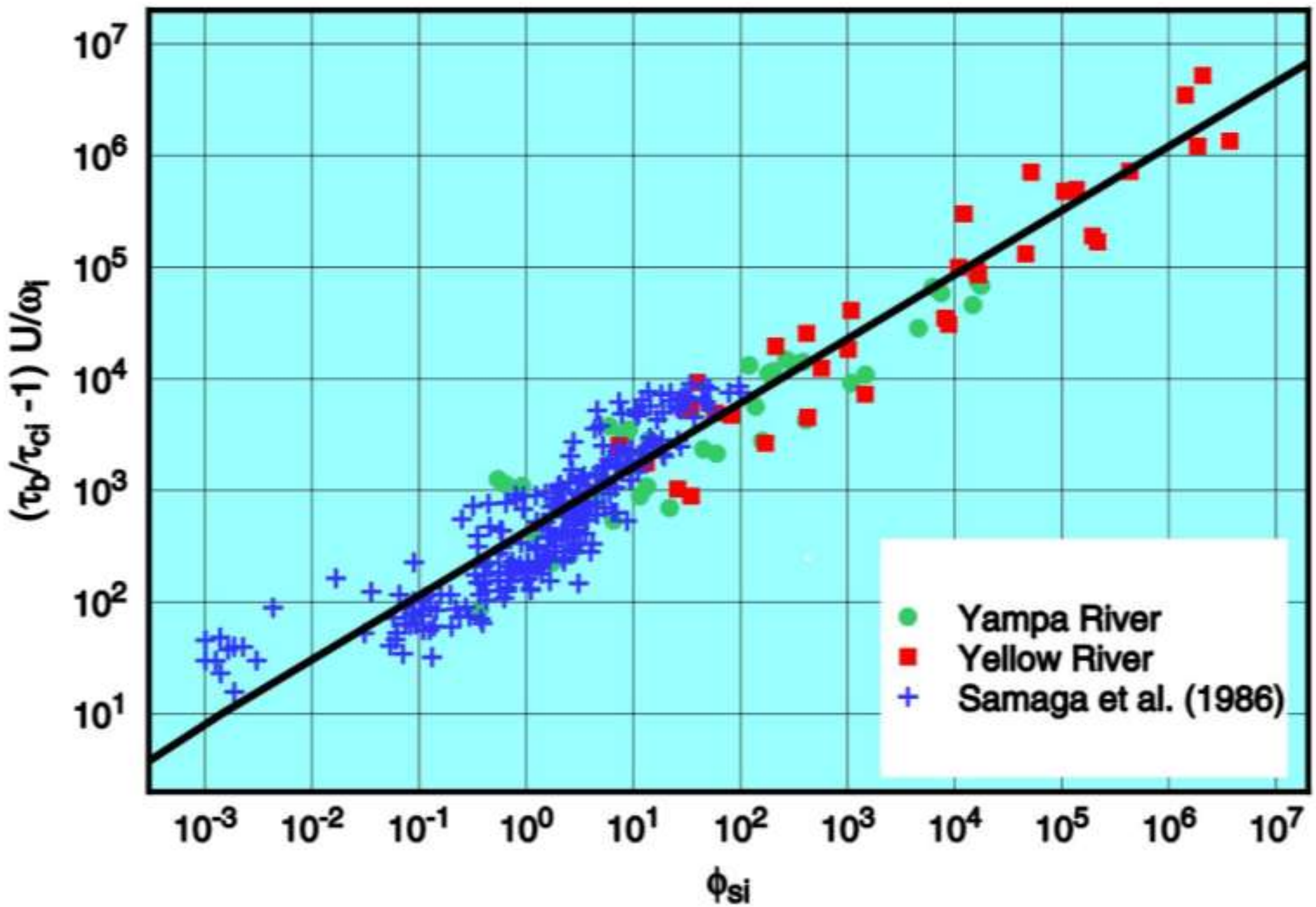

$$\frac{q_{sk}}{p_{bk}\sqrt{\left(\gamma_s/\gamma - 1\right) g d_k^3}} = 0.0000262\left[\left(\frac{\tau}{\tau_{ck}} - 1\right)\frac{U}{\omega_{sk}}\right]^{1.74}$$

Reliable Transport Capacity Formulas

Clarkson UNIVERSITY defy convention

Single-sized total load

Ackers-White (1973) formula is good for coarse sediment, not for fine sediment

Laursen (1958) formula is good for fine sand and silt, not for coarser sediment

Yang's (1973, 1984) formula has two sets of coefficients for sand and gravel

Wu et al. (2000) and Engelund-Hansen (1967) are good for wider size ranges

Sing-sized bed load

Wu et al. (2000) formula

Meyer-Peter and Mueller (1948) formula

Single-sized suspended load

Zhang (1961) formula

Multiple-sized total load

Wu et al. (2000) formula is the top choice

*: Ultimately, calibration using measurements is the most reliable approach.

Bed Material Sorting

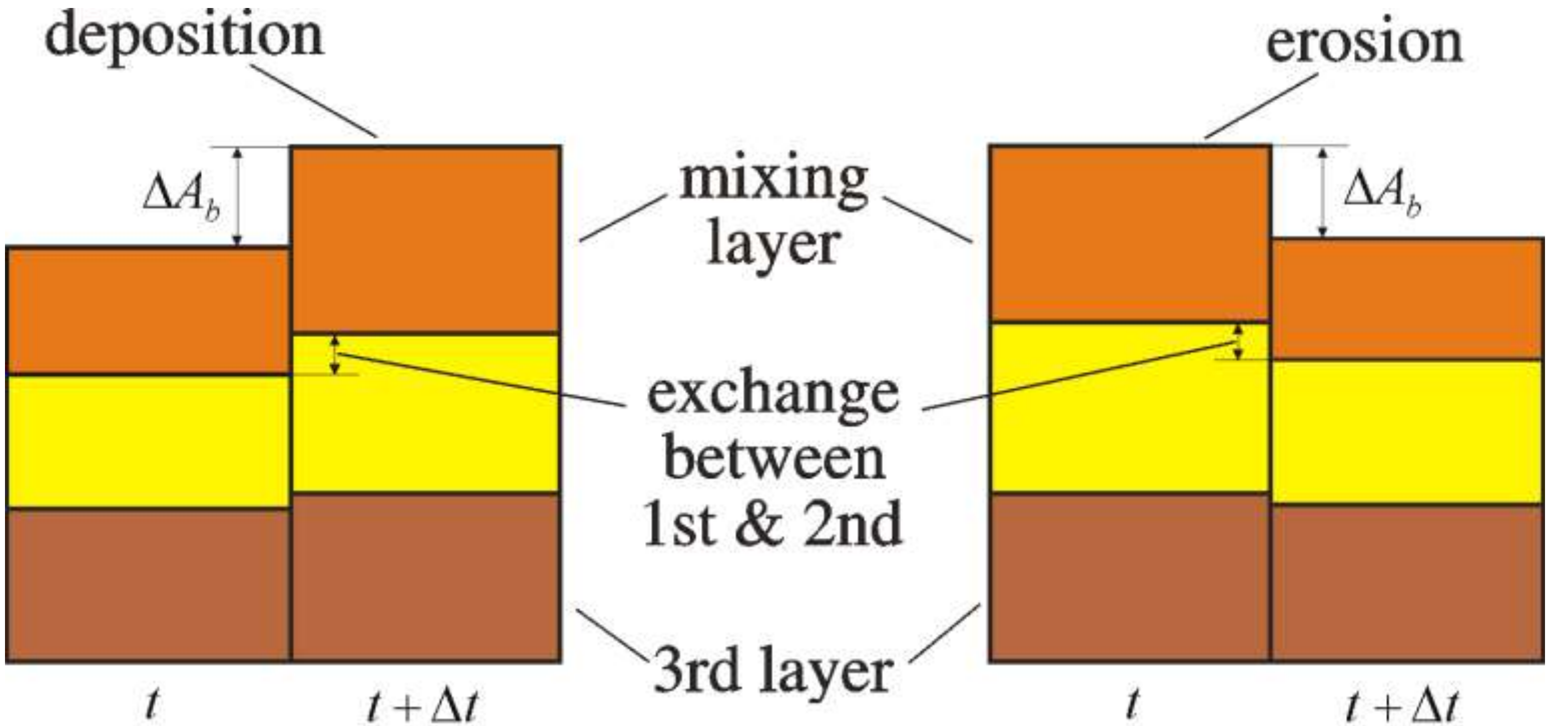

Bed Material Composition in Mixing Layer:

$$\frac{\partial(\delta_m p_{bk})}{\partial t} = \frac{\partial z_{bk}}{\partial t} + p_{bk}^* \left(\frac{\partial \delta_m}{\partial t} - \frac{\partial z_b}{\partial t} \right)$$

Bank Erosion

- Planar Failure Method (Osman and Thorne, 1988)

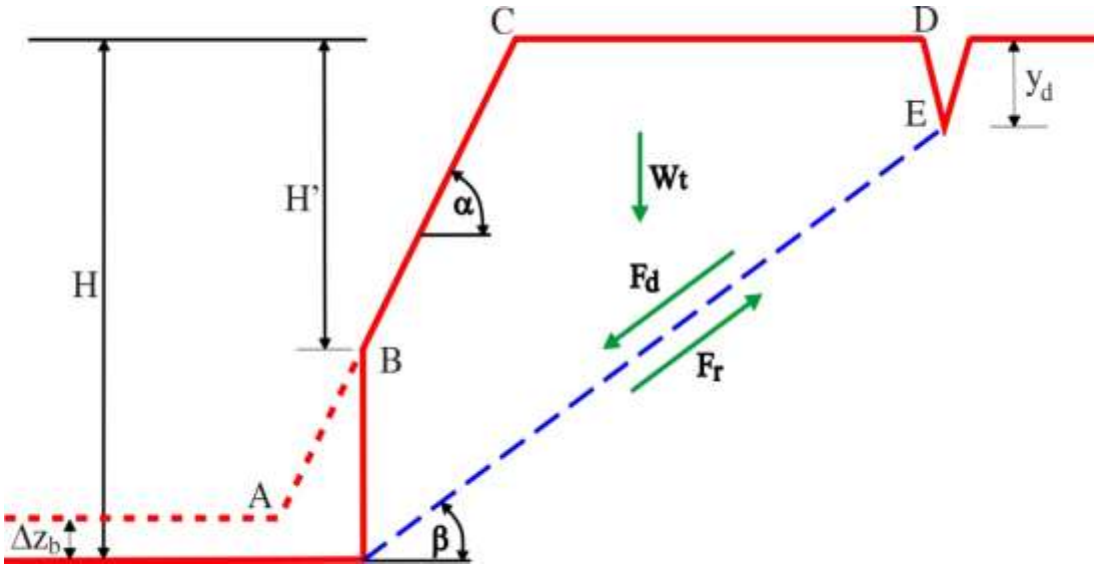

$$f_s = \frac{F_r}{F_d}$$

$$F_d = W_t \sin\beta = \frac{\gamma_s}{2}\left(\frac{H^2 - y_d^2}{\tan\beta} - \frac{H'^2}{\tan\alpha}\right)\sin\beta$$

$$F_r = \frac{(H - y_d)C}{\sin\beta} + \frac{\gamma_s}{2}\left(\frac{H^2 - y_d^2}{\tan\beta} - \frac{H'^2}{\tan\alpha}\right)\cos\beta\tan\varphi$$

CCHE1D Simulation Results

Channel Degradation (Newton, 1951)

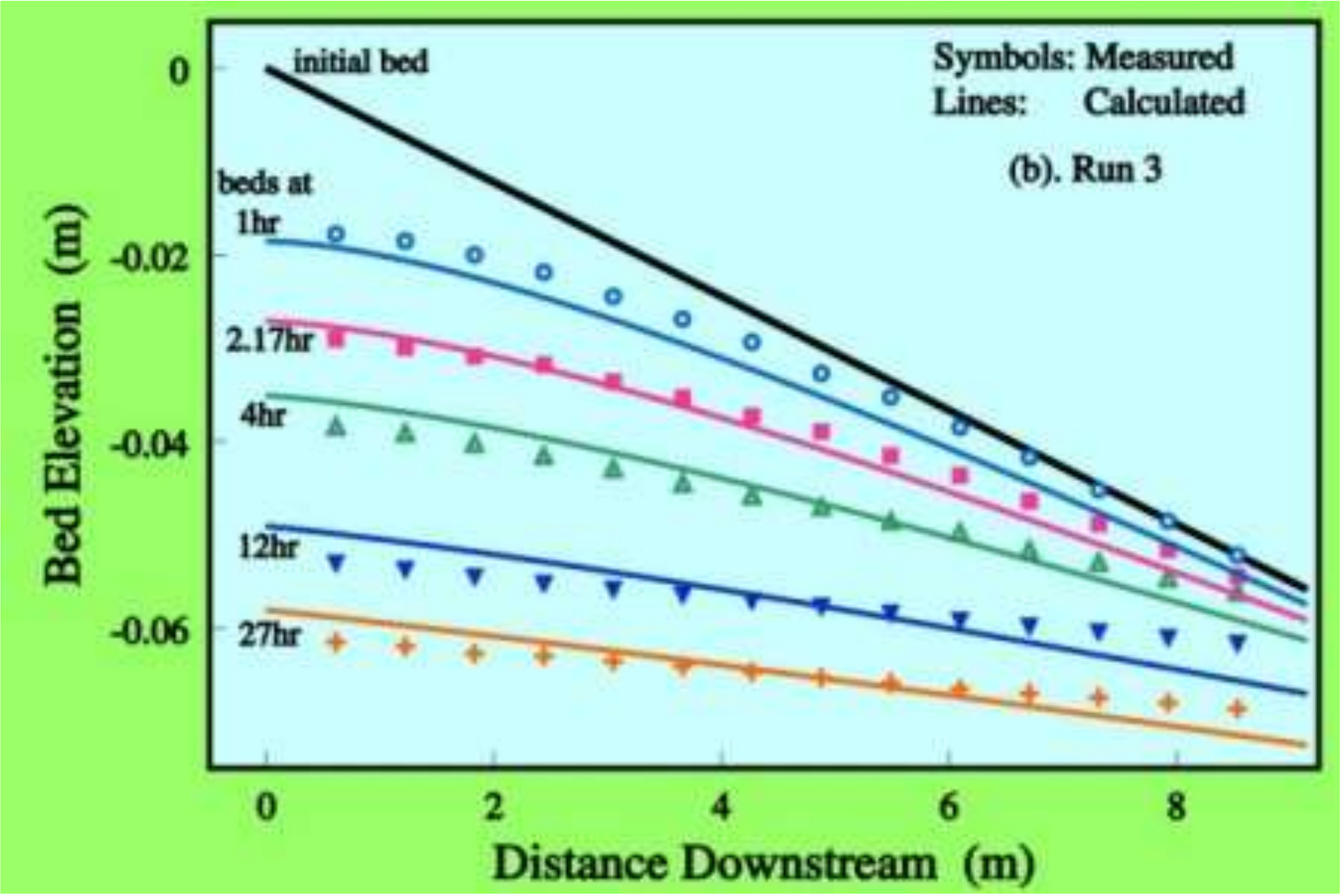

Degradation using Different *L*

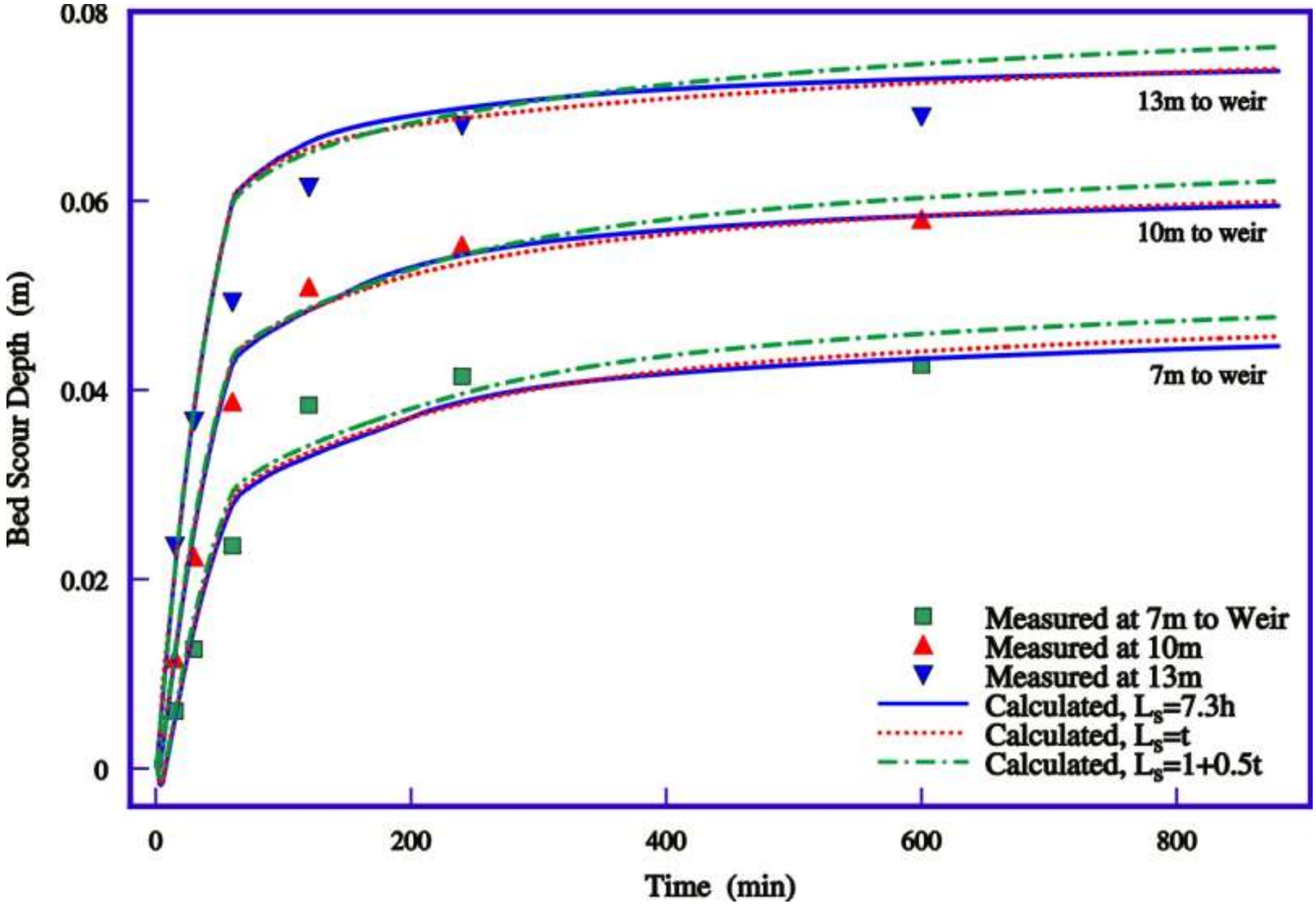

Degradation using Different Mixing Layer Thickness

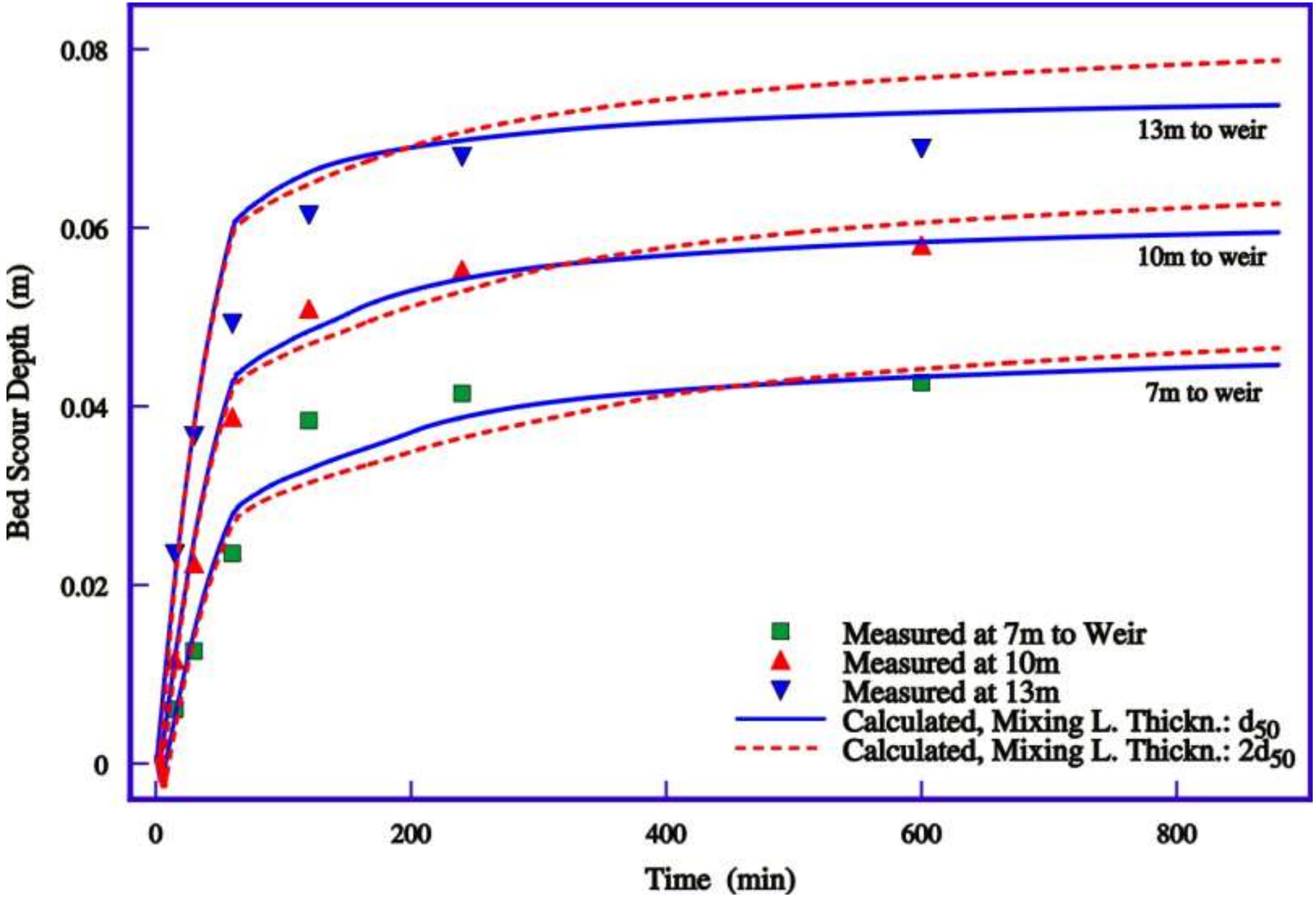

Channel Aggradation

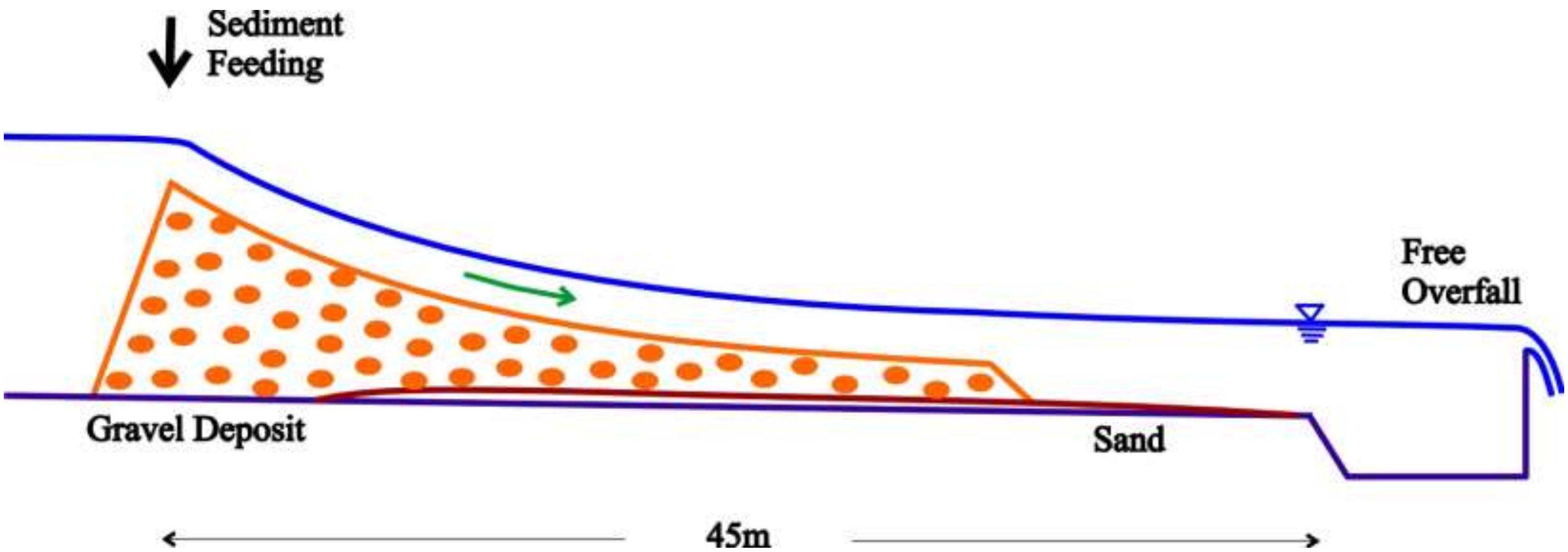

Configuration of Experiment (SAFHL, 1995)

Size Classes

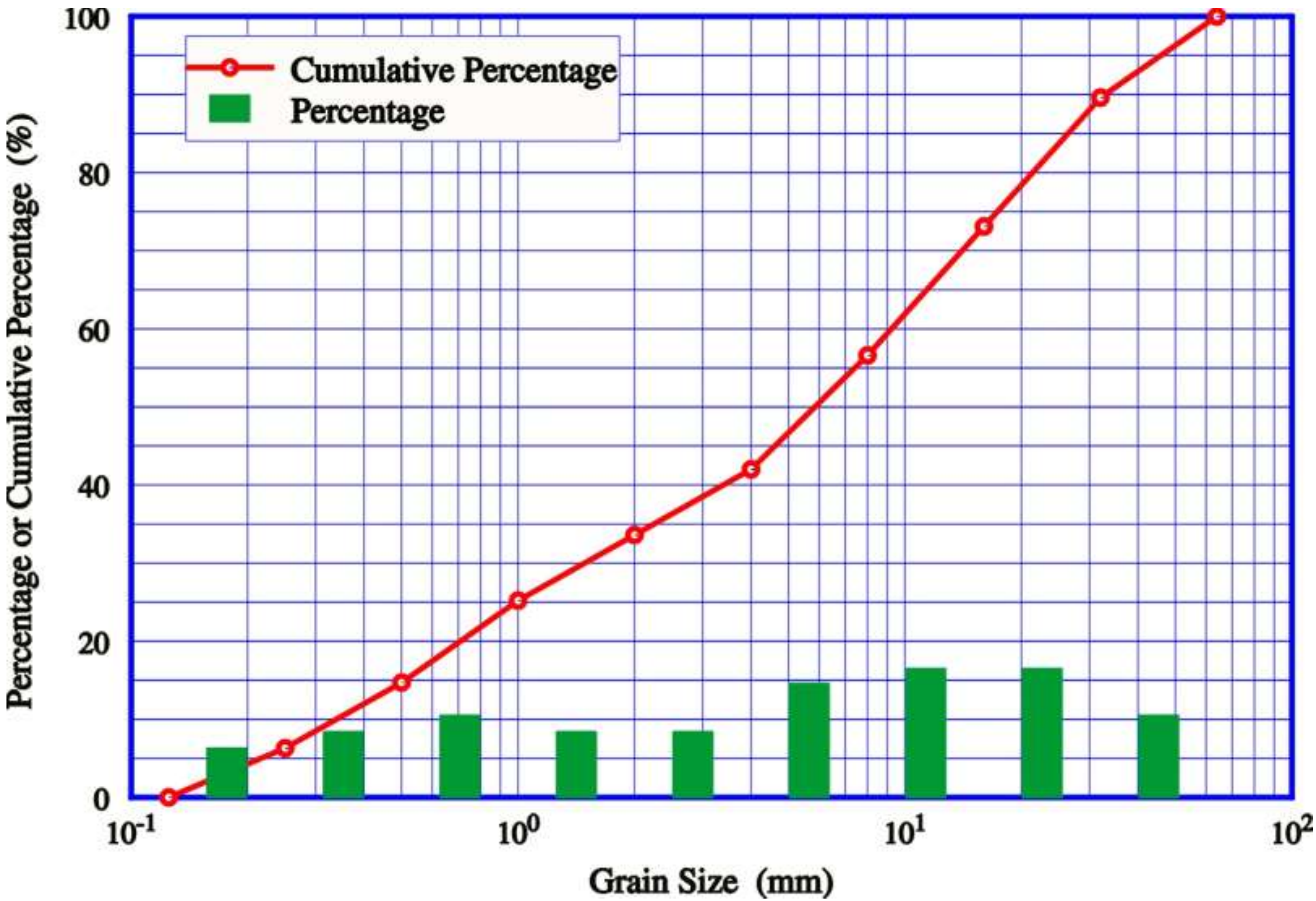

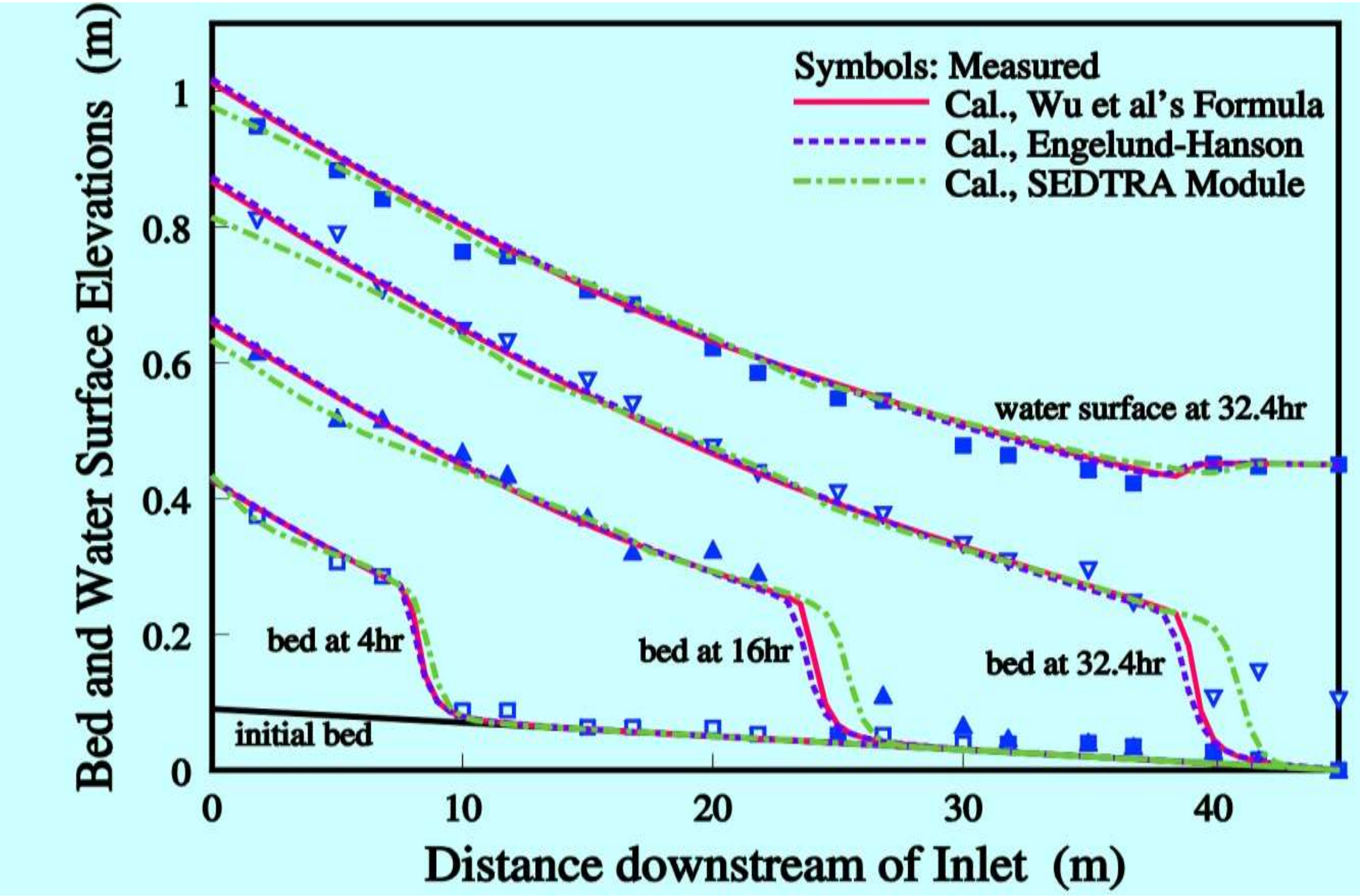

Bed and Water Surface Elevations (m)
Distance downstream of Inlet (m)
0
0.2
0.4
0.6
0.8
1
0
10
20
30
40
Symbols: Measured
Cal., Wu et al's Formula
Cal., Engelund-Hanson
Cal., SEDTRA Module
water surface at 32.4hr
bed at 4hr
bed at 16hr
bed at 32.4hr
initial bed

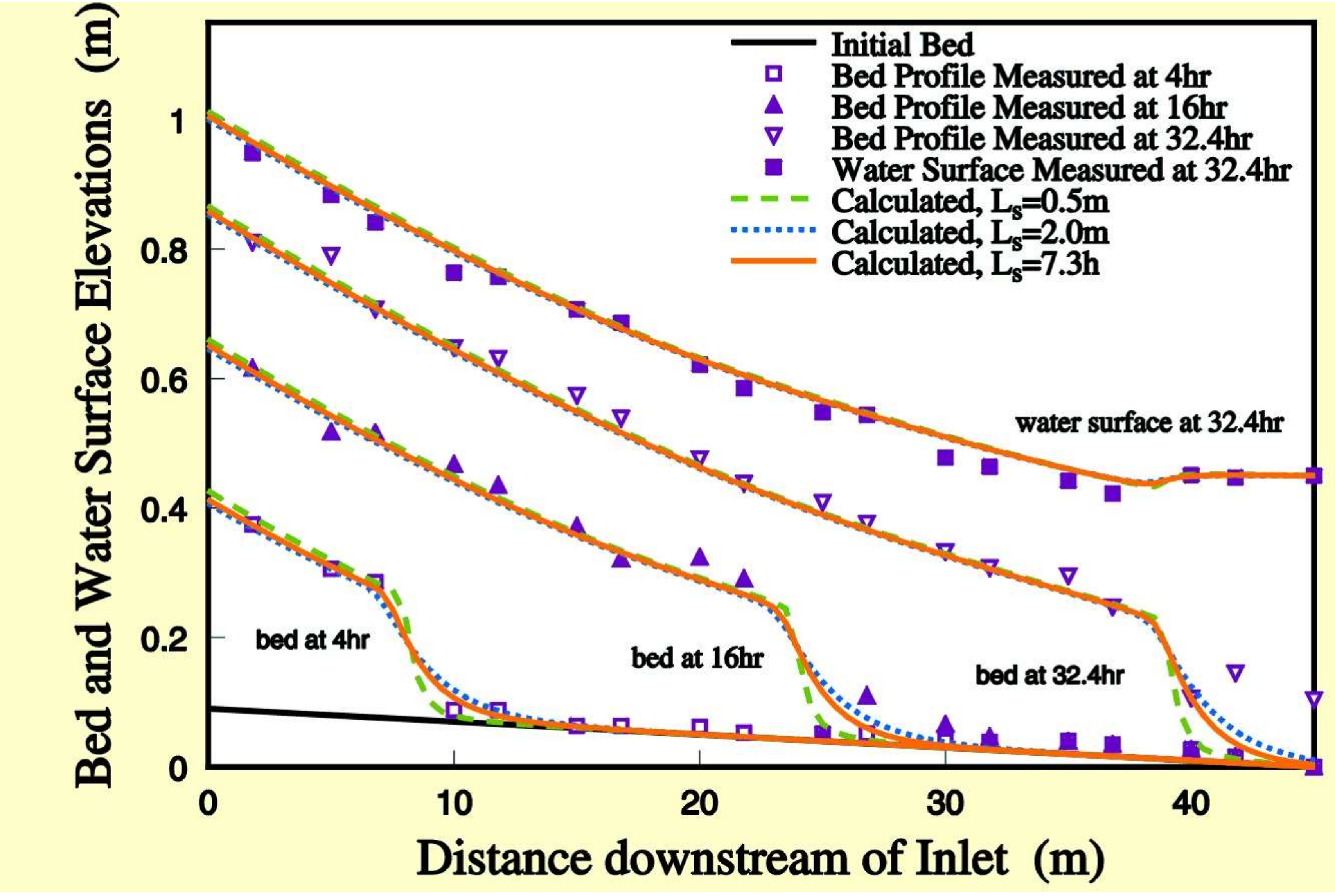

Bed and Water Surface Elevations (m)
0
0.2
0.4
0.6
0.8
1
0
10
20
30
40
Distance downstream of Inlet (m)
Initial Bed
Bed Profile Measured at 4hr
Bed Profile Measured at 16hr
Bed Profile Measured at 32.4hr
Water Surface Measured at 32.4hr
Calculated, Ls=0.5m
Calculated, Ls=2.0m
Calculated, Ls=7.3h
water surface at 32.4hr
bed at 4hr
bed at 16hr
bed at 32.4hr

In-stream Hydraulic Structures

Measuring flume in Goodwin Creek, MS

DEC Low Drop Structure

Erosion in Pa-Chang River

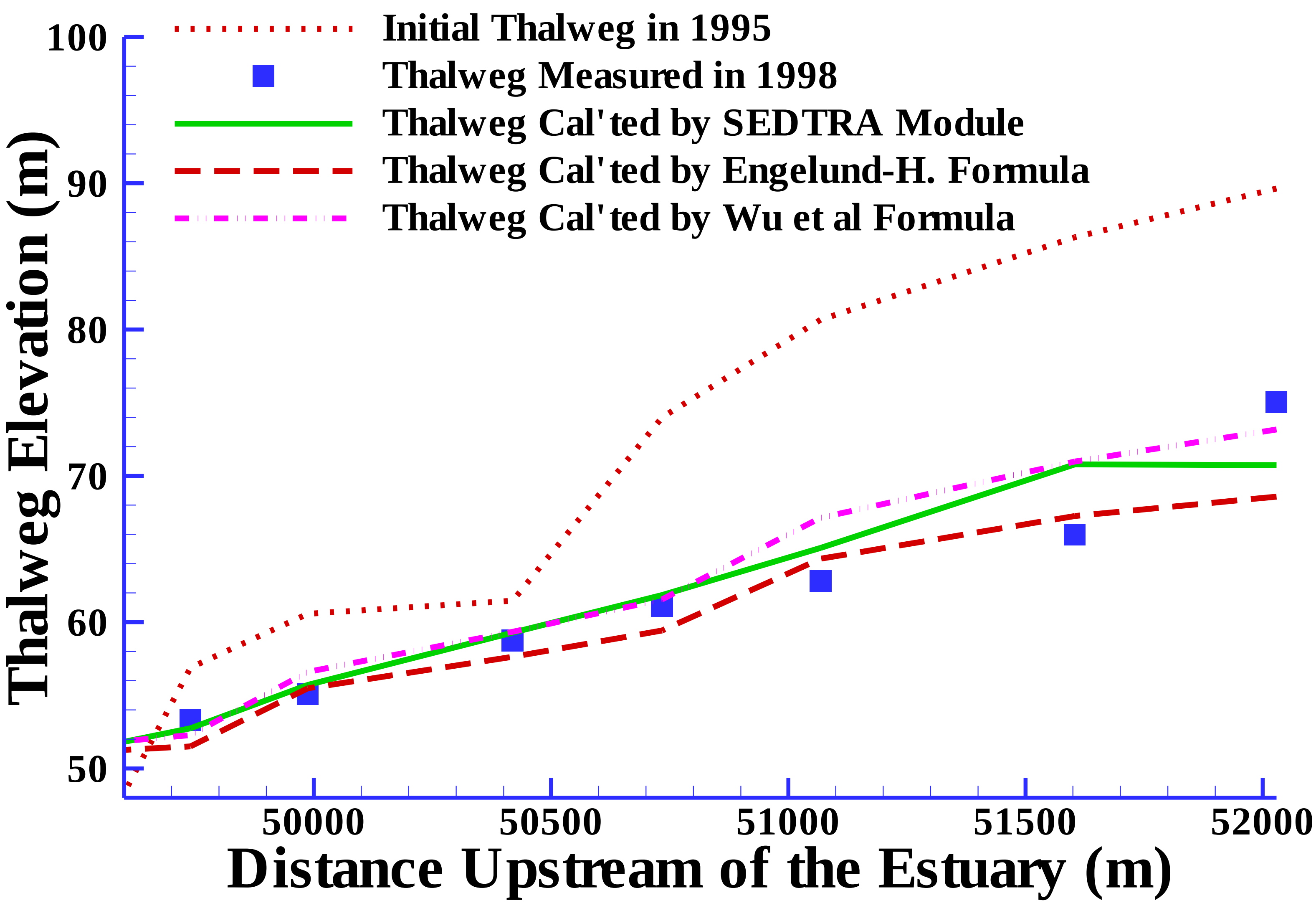

Erosion Control Analysis

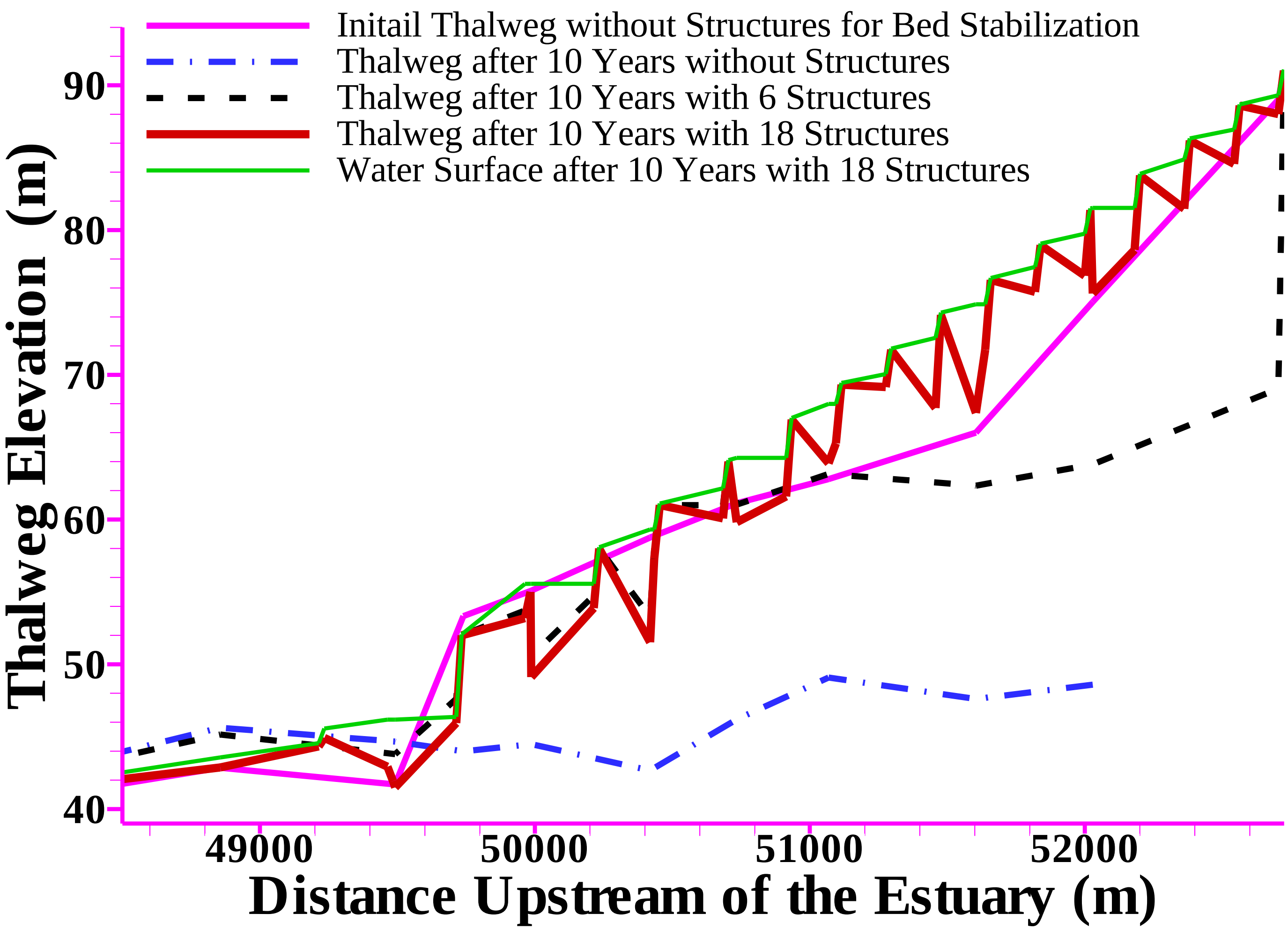

Danjiangkou Reservoir in Han River, China

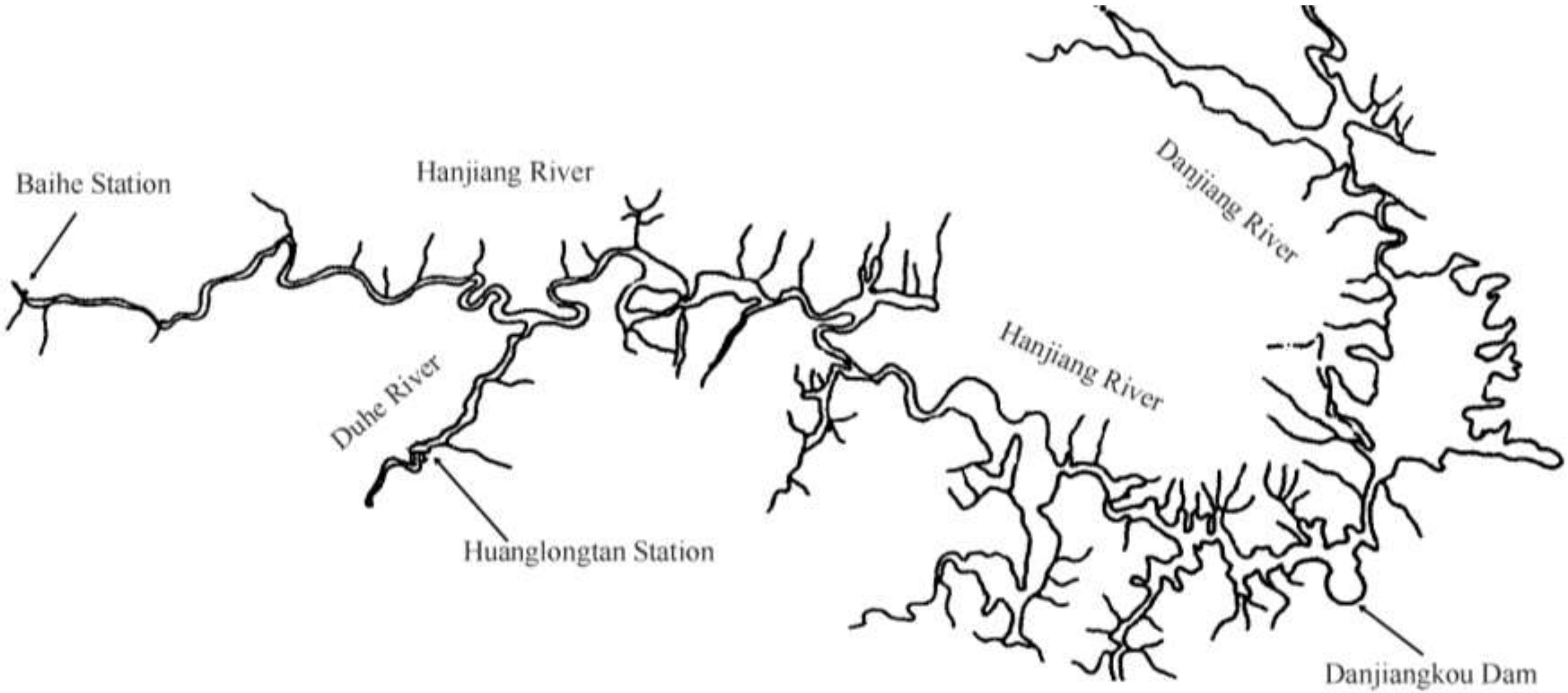

Annual Sediment Deposition in Danjiangkou Reservoir

Clarkson University defy convention

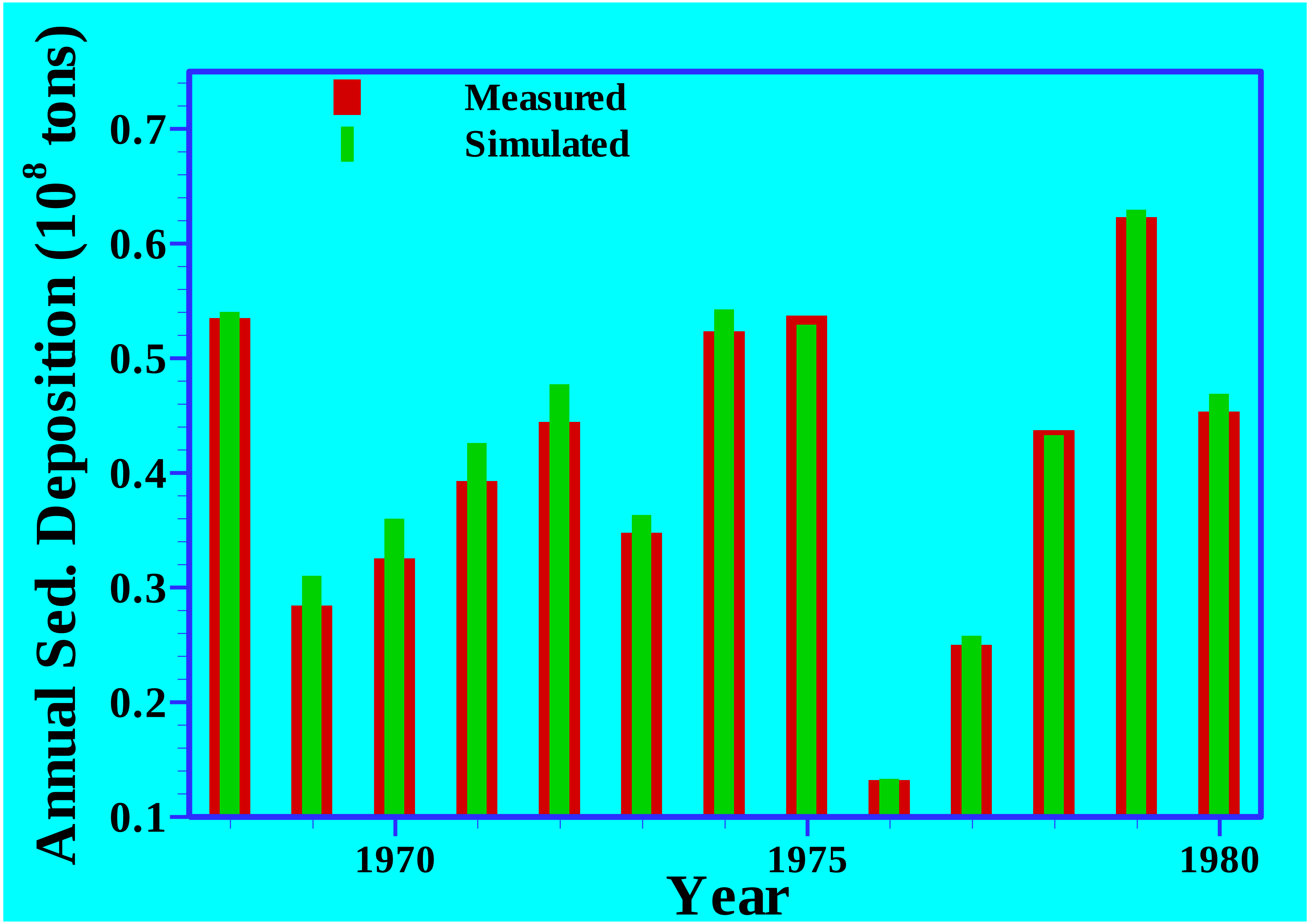

Deposition Profile in Danjiangkou Reservoir

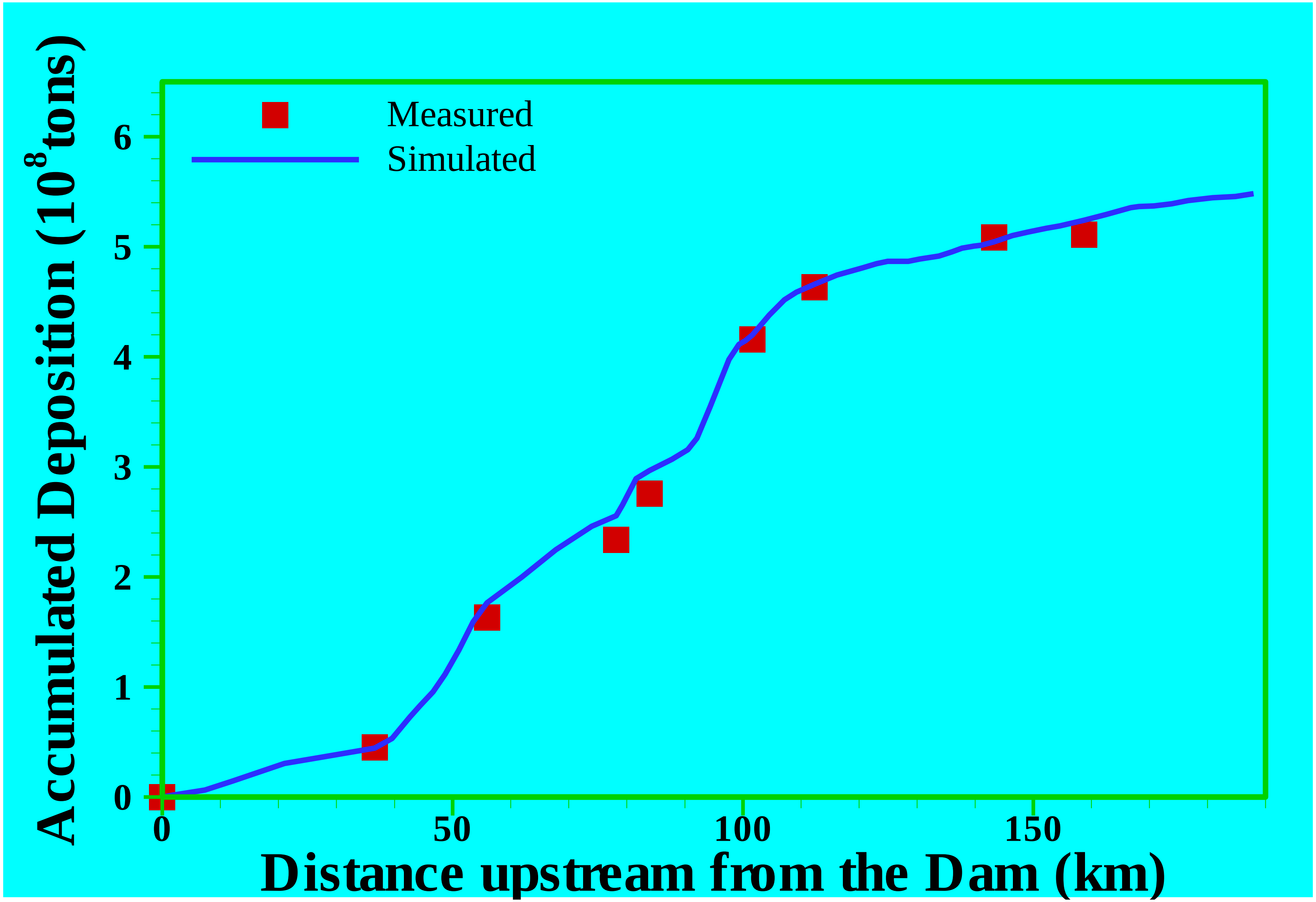

Three Gorges Reservoir

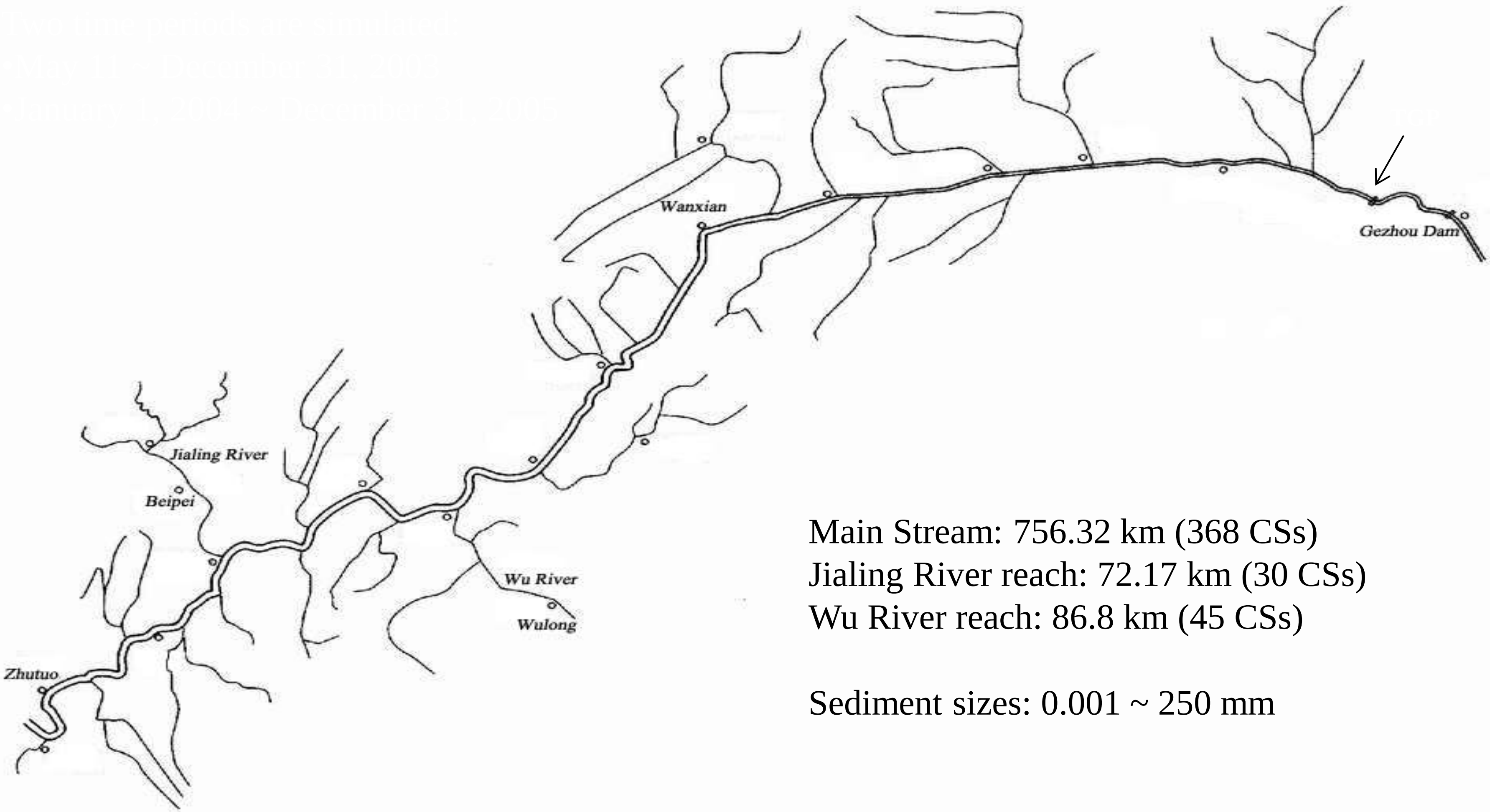

Main Stream: 756.32 km (368 CSs)
Jialing River reach: 72.17 km (30 CSs)
Wu River reach: 86.8 km (45 CSs)

Sediment sizes: 0.001 ~ 250 mm

Three Gorges Reservoir (Cont'd)

- **Jan 1, 2004 ~ Dec 31, 2005**

- **Station:**

  Cuntan **(604.12 km to the dam)**

  Qingxichang **(479.3 km to the dam)**

  Wanxian **(291.61 km to the dam)**

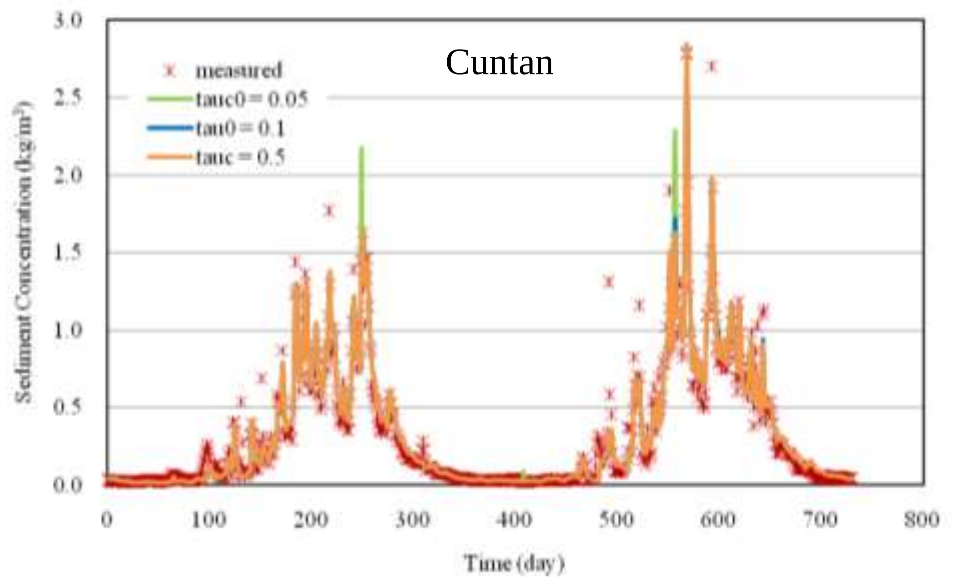

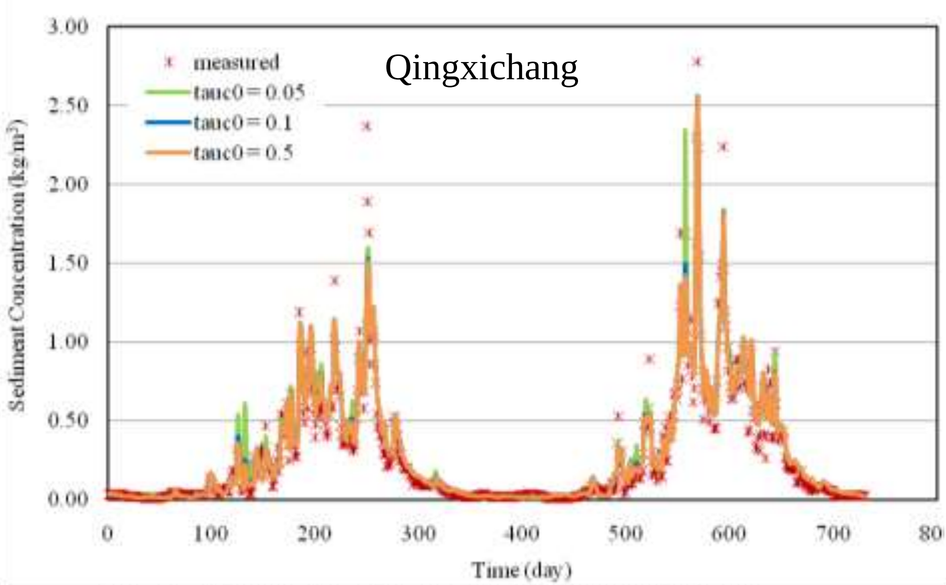

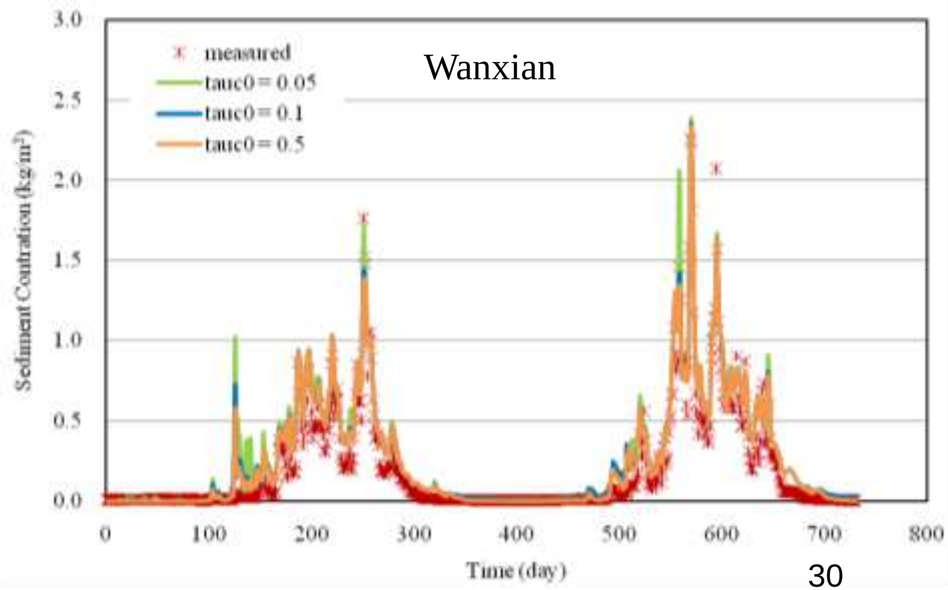

FASTER2D Simulation Results

Flow in Gangjiang River with Multiple Dikes

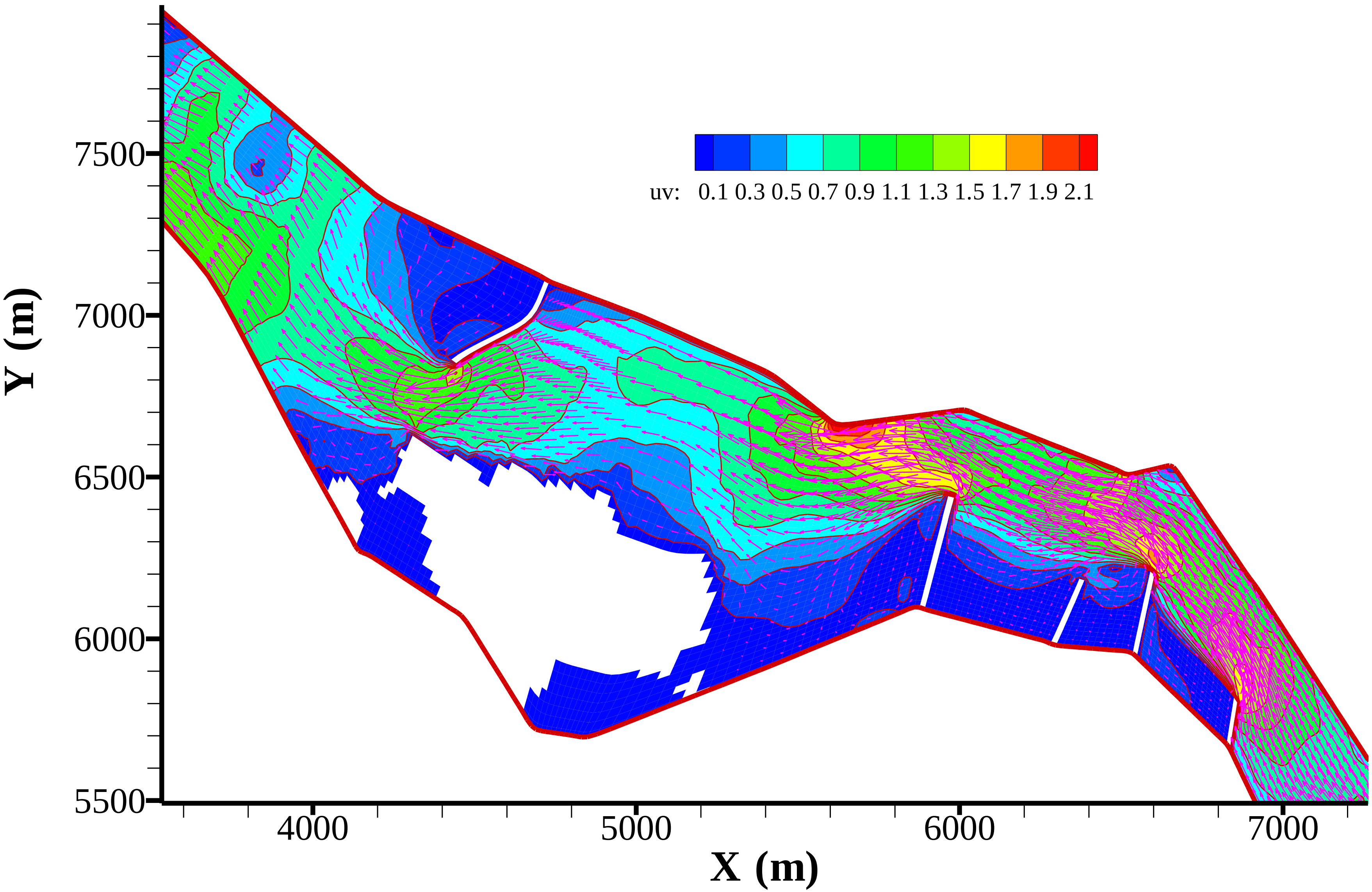

Hysteresis of Flow and Sediment Transport

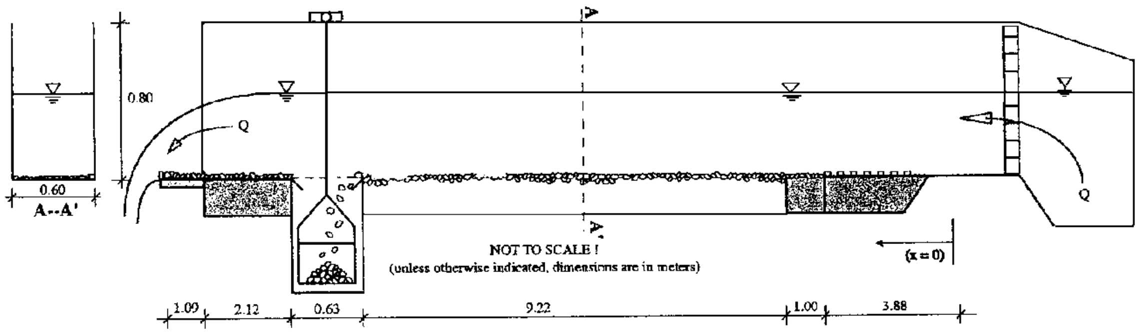

Configuration of Qu's (2003) experimental setup

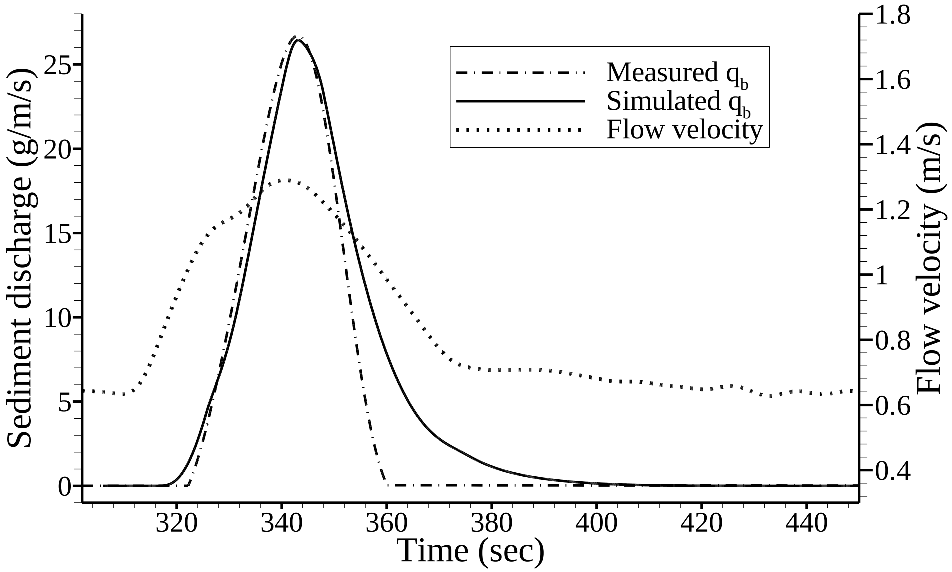

Measured vs. calculated bed-load discharges
(Run TM07)

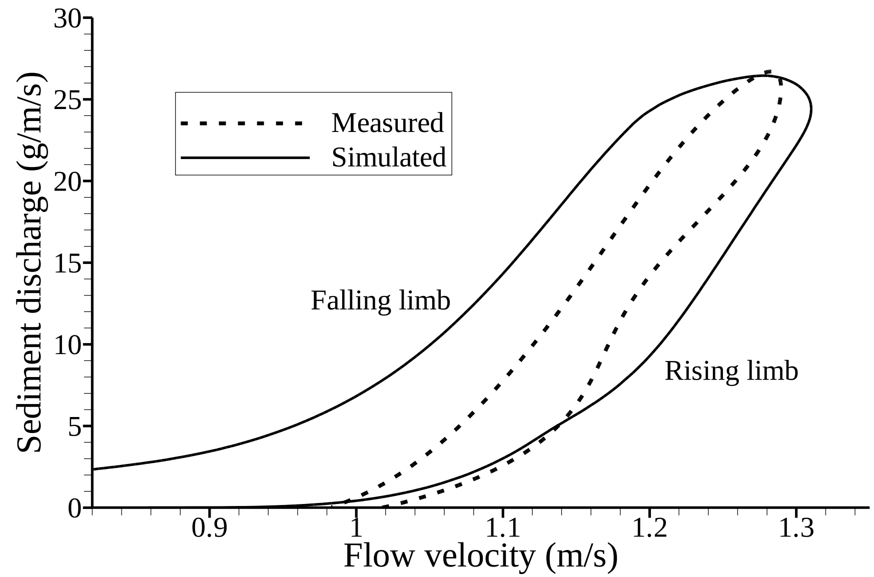

Relation of bed-load discharge and flow velocity
(Run TM07)

High Flow during 1996 Flood in Lower Yellow River (90 km Long)

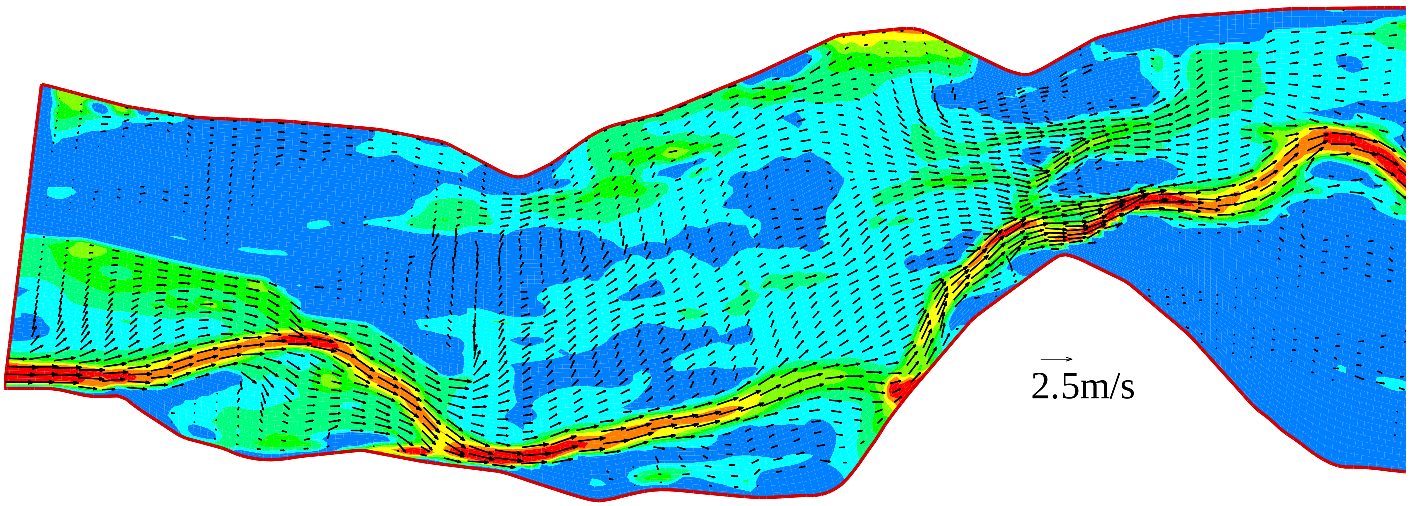

Huayuankou - Dazhangzhuang

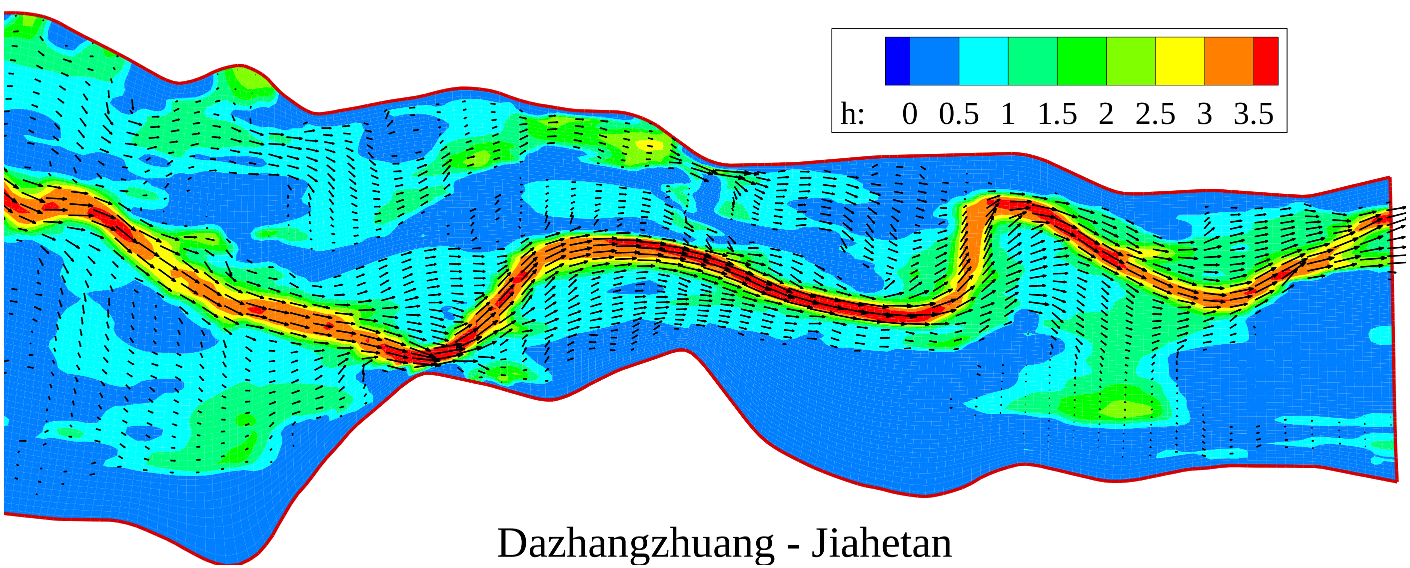

Dazhangzhuang - Jiahetan

Low Flow during 1996 Flood in Lower Yellow River (90 km Long)

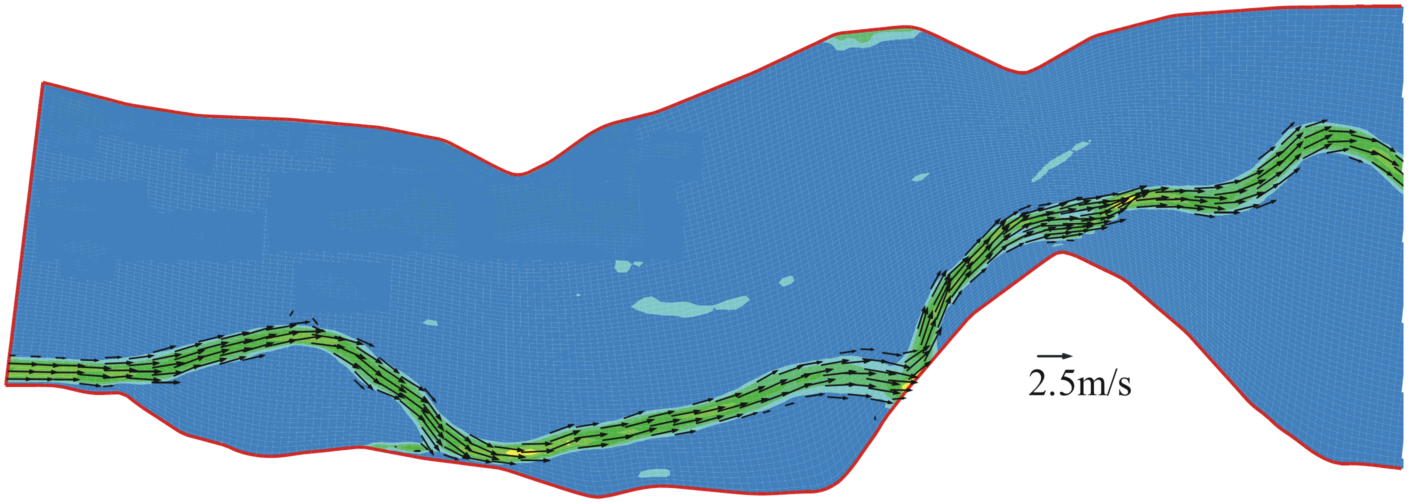

Huayuankou - Dazhangzhuang

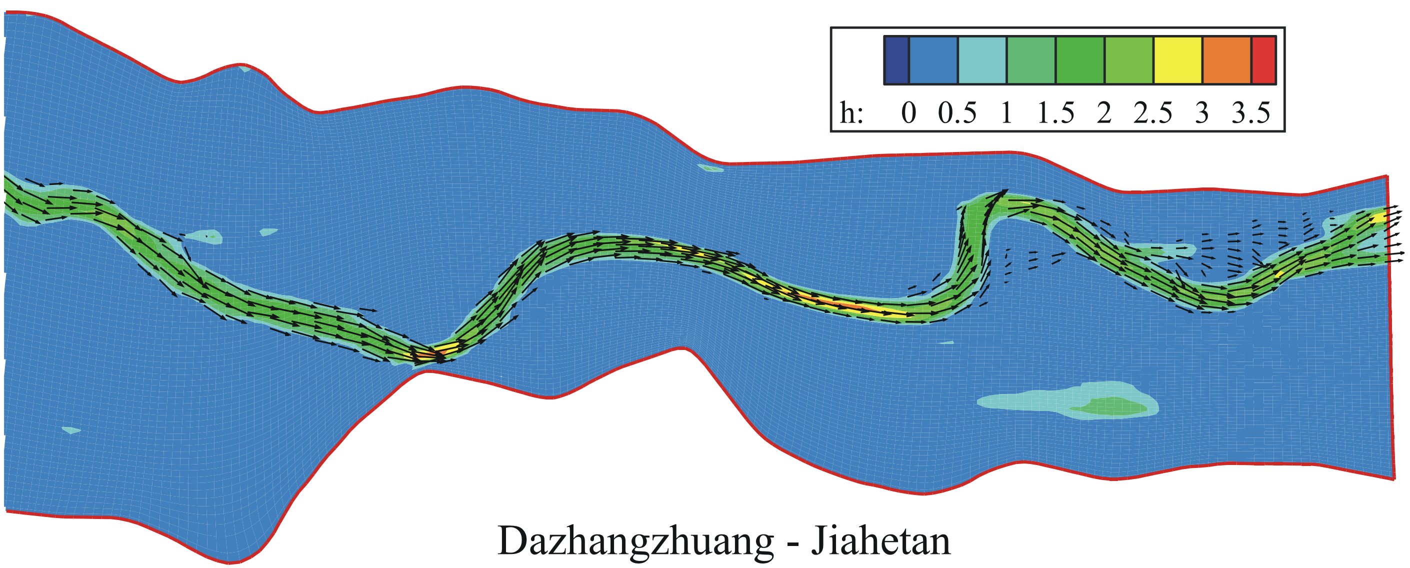

Dazhangzhuang - Jiahetan

Flow Discharge in Lower Yellow River during 1982 Flood

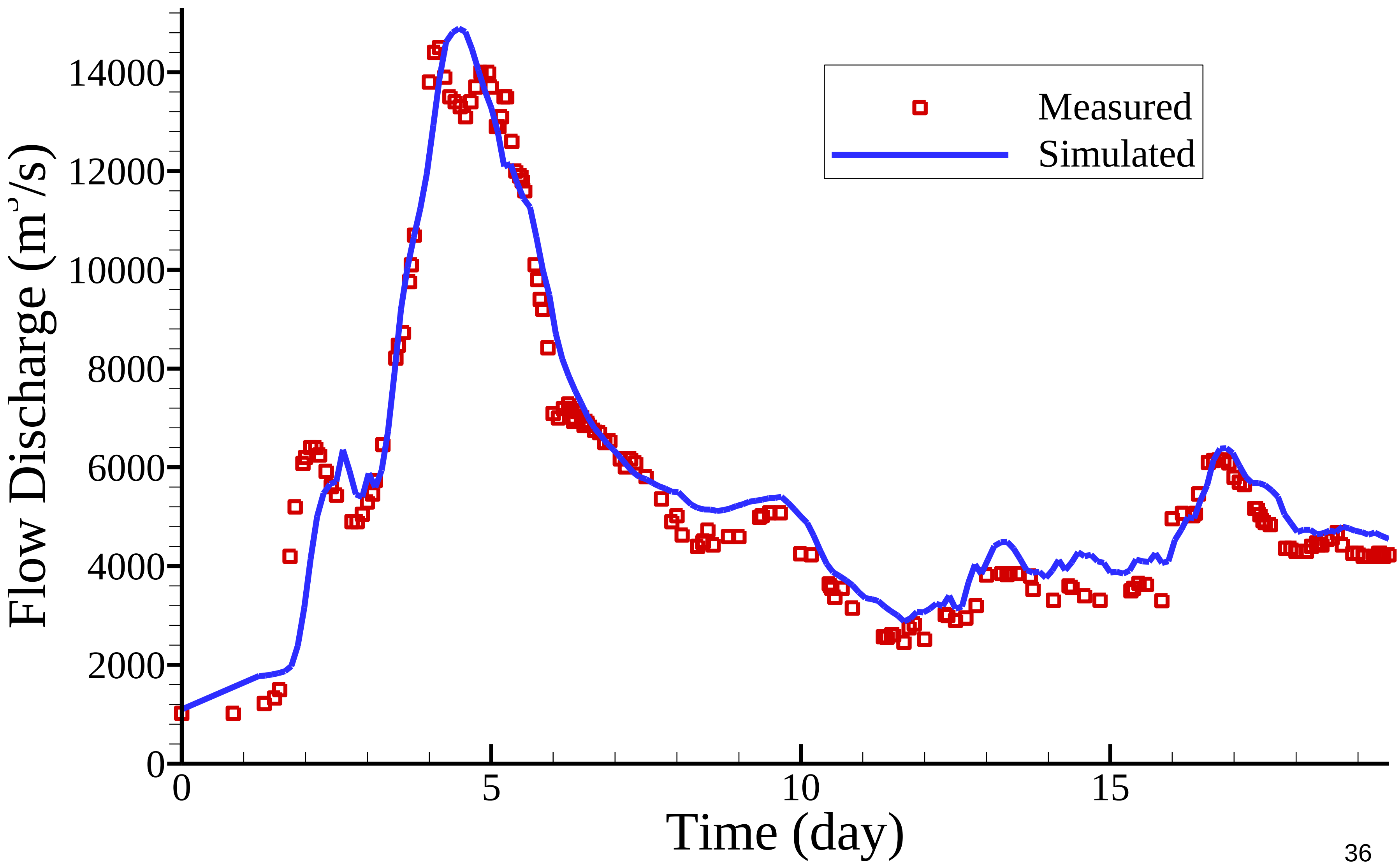

Sediment Concentration in Lower Yellow River during 1982 Flood

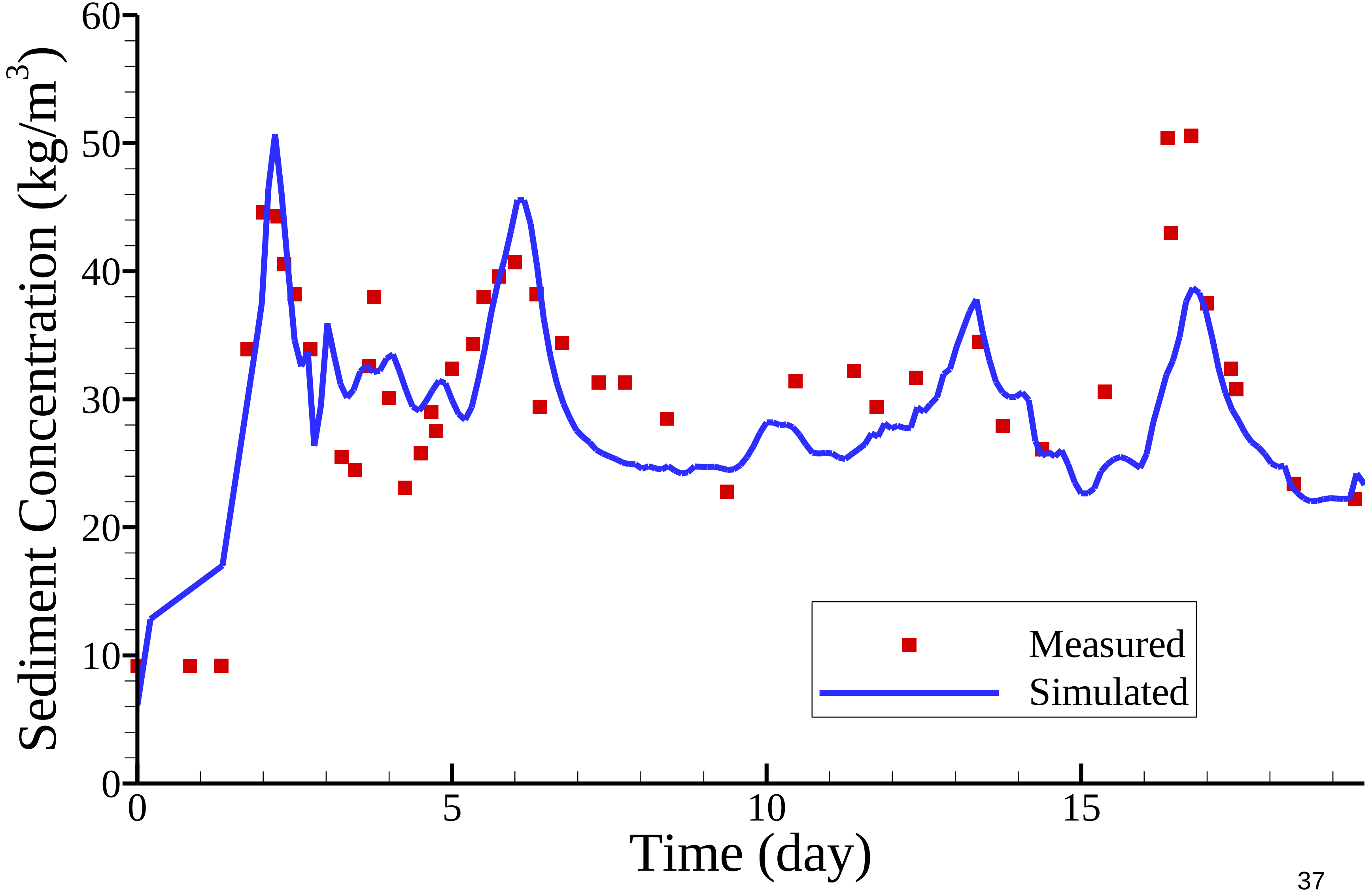

Water Surface Contours in the Study Reach of East Fork River

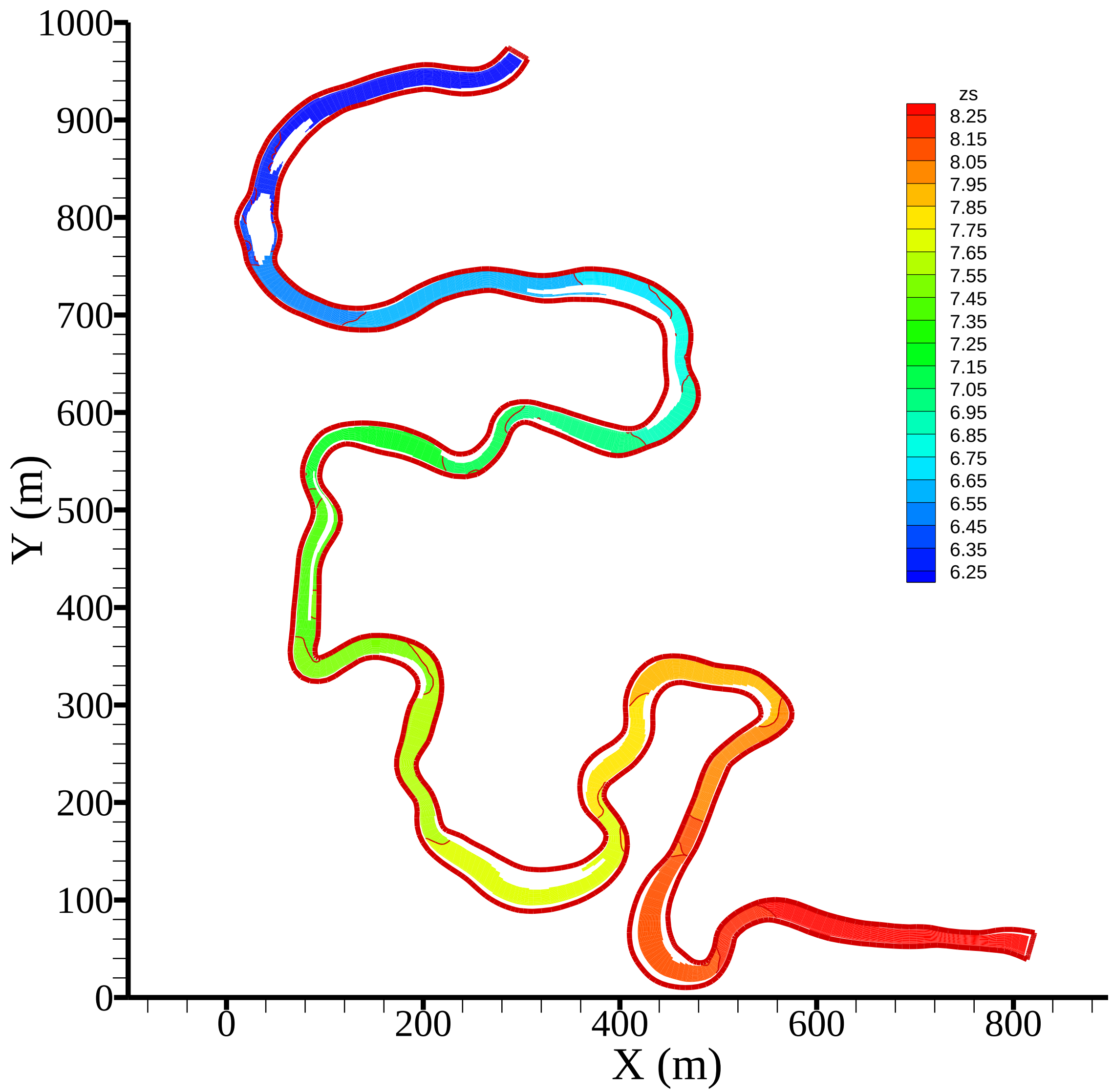

Flow Field in a Bend of the East Fork River

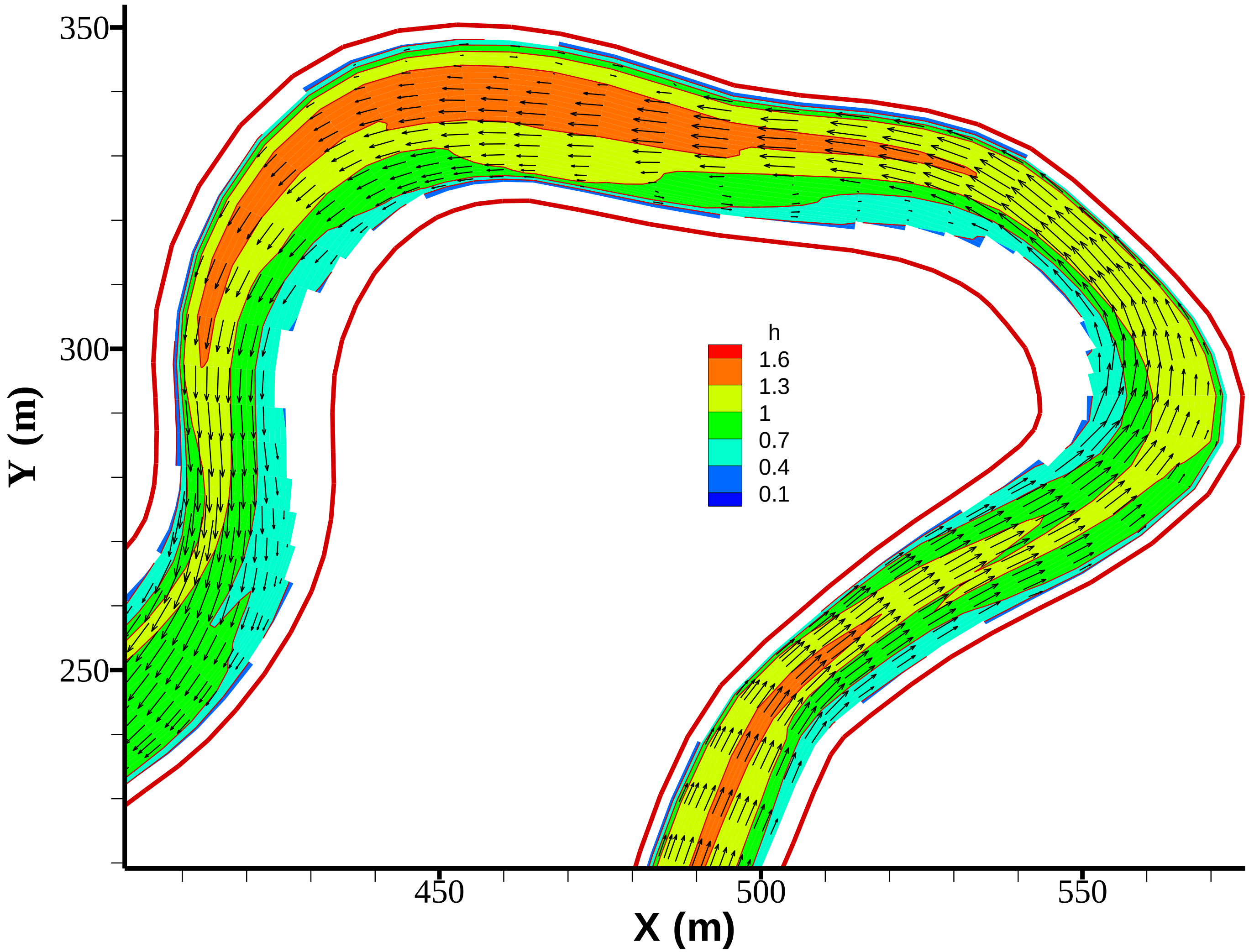

Flow Discharge at Outlet in the Study Reach of the East Fork River

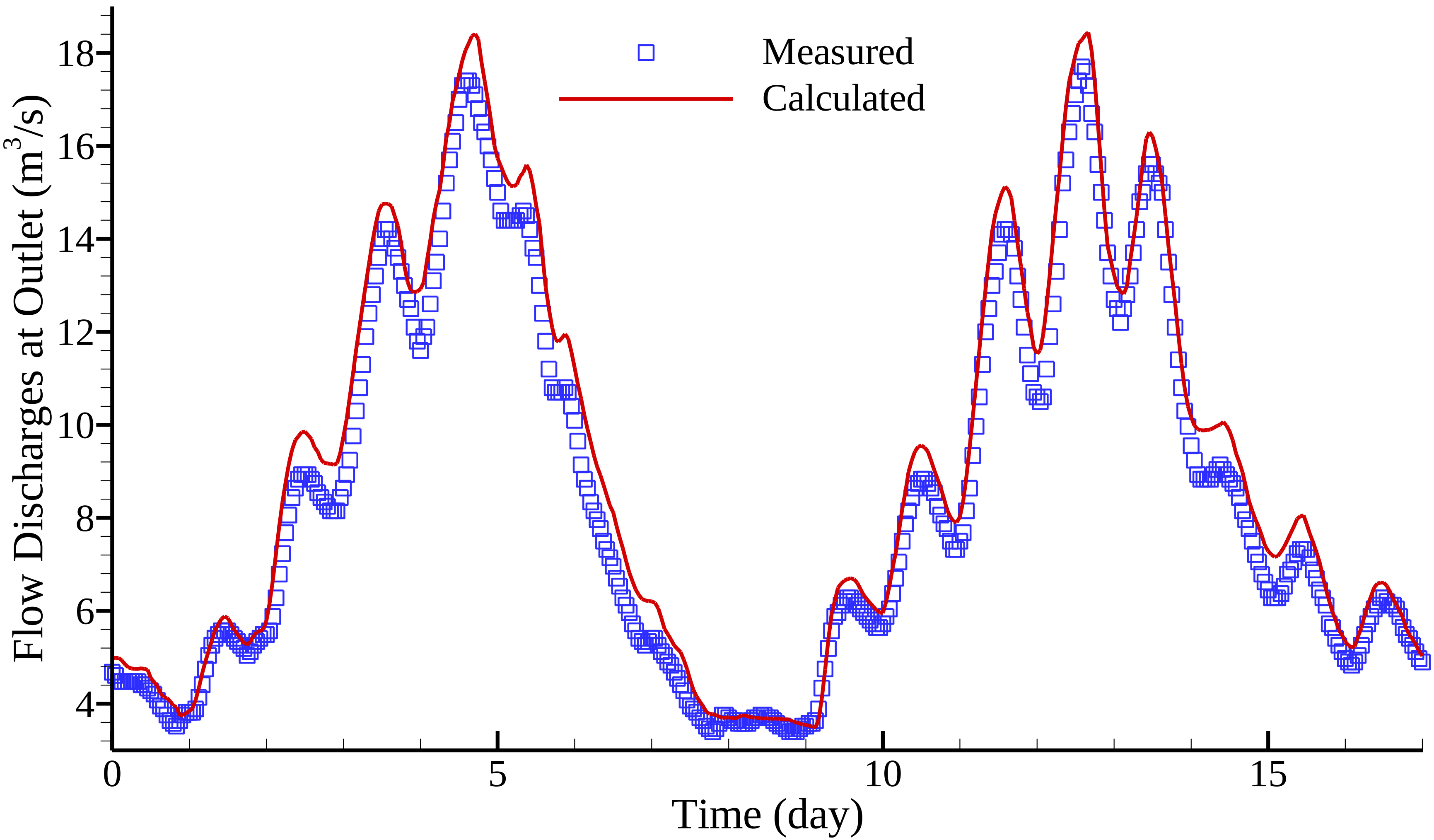

Sediment Discharge at Outlet in the Study Reach of the East Fork River

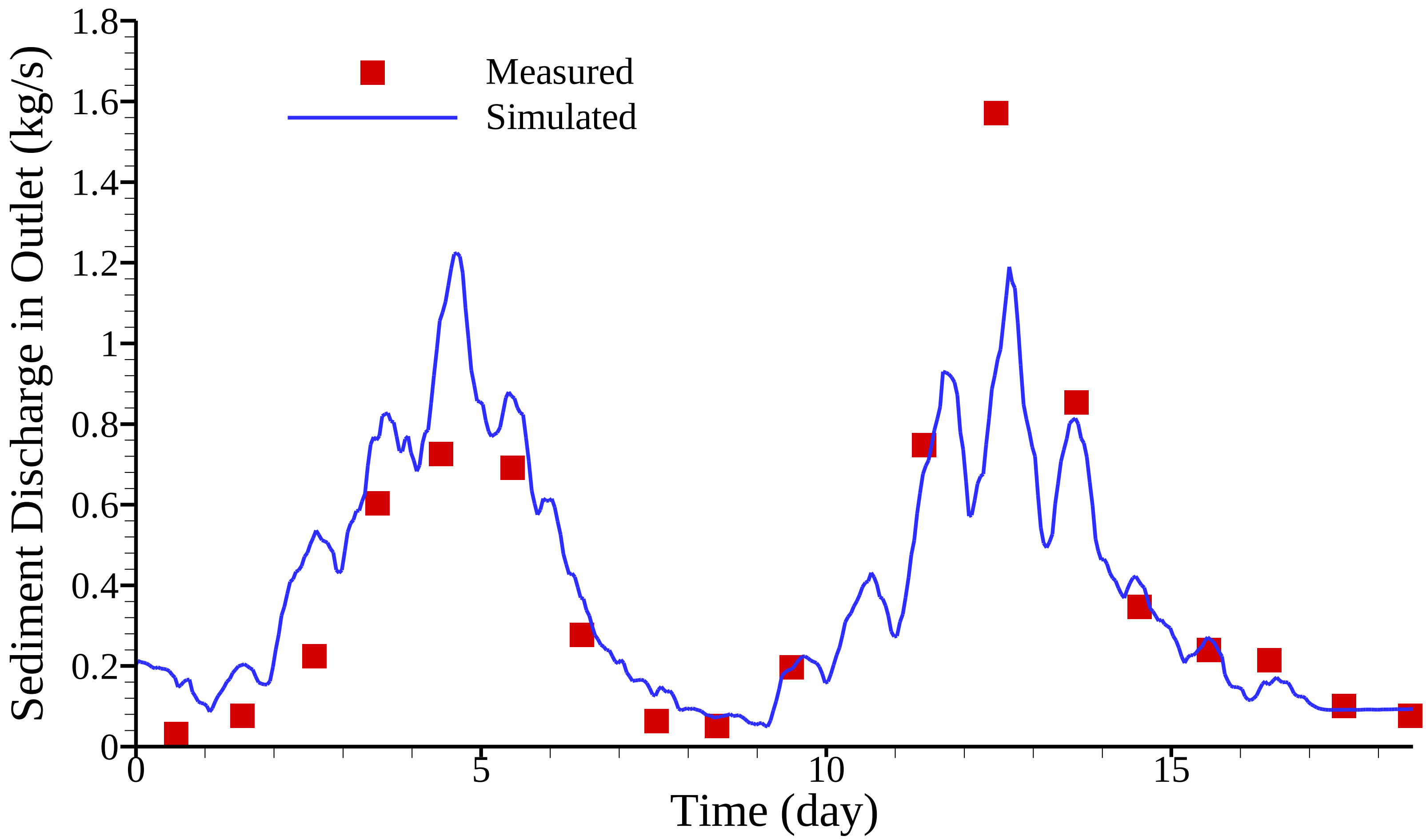

Helical Flow

Transversal velocity – linear model:

$$u_n = U_n + b_s I\left(\frac{2z}{h} - 1\right)$$

At channel centerline $I = U_s h / r$

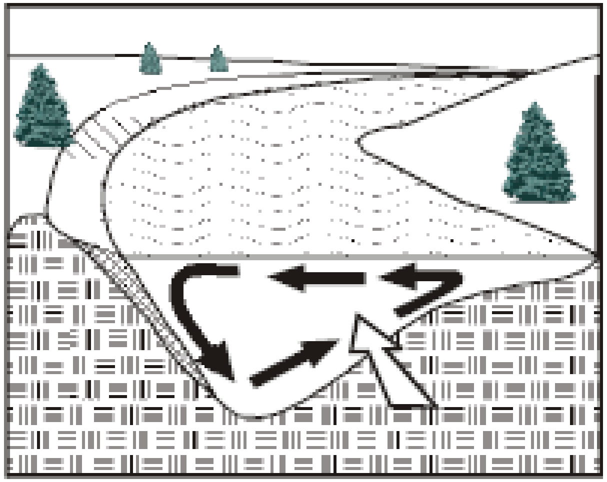

Distribution of I in a cross section:

$$\frac{rI}{\beta_I h U_s} = 1 - \frac{1 - e^{-B/\sqrt{T_a D_I}}}{e^{B/\sqrt{T_a D_I}} - e^{-B/\sqrt{T_a D_I}}} e^{B\eta/\sqrt{T_a D_I}} - \frac{e^{B/\sqrt{T_a D_I}} - 1}{e^{B/\sqrt{T_a D_I}} - e^{-B/\sqrt{T_a D_I}}} e^{-B\eta/\sqrt{T_a D_I}}$$

where U_s and U_n are the depth-av. velocities in streamwise and lateral directions, β_I is a coefficient determining the magnitude of I, T_a is the adaptation time scale, D_I is the dispersion coefficient, and η is the dimensionless distance in lateral direction (Wu and Wang, 2004).

An example distribution of I is shown in the figure.

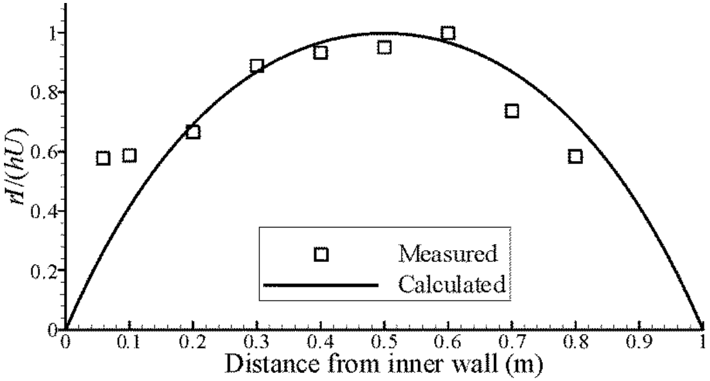

Transport Angle of Bed Load

Helical flow effect:

Engelund (1974)

$$\tan \delta_b = 7\frac{h}{r}$$

where δ_b is the angle between bed-load and the main flow direction

Odgaard (1986)

$$\tan\delta_b = \frac{v_b}{u_b}$$

where u_b and v_b are the near-bed flow velocities in the x and y directions

Transport Angle of Bed Load

Bed slope effect:

Parker (1984)

$$\frac{q_{bn}}{q_{bs}} = \tan\delta_b + \frac{1+\alpha_p\mu_c}{\lambda_s\mu_c}\sqrt{\frac{\Theta_c}{\Theta}}\tan\varphi$$

where φ is the lateral inclination of the bed, and Θ is the Shields number.

Struiksma et al. (1985) and Sekine and Parker (1992)

$$\frac{q_{bn}}{q_{bs}} = \tan\delta_b - \beta_b\frac{\partial z_b}{\partial n}$$

where z_b is the bed level, n is the lateral direction, and βb is a coefficient.

Wu (2004)

$$\frac{\alpha_{bx,e}}{\alpha_{by,e}} = \frac{\tau_b'\alpha_{bx} + \lambda_0\tau_c\sin\varphi_x/\sin\phi_r}{\tau_b'\alpha_{by} + \lambda_0\tau_c\sin\varphi_y/\sin\phi_r}$$

where φ is bed slope angle and ϕ_r is the repose angle.

Dispersion of Suspended Load

Longitudinal velocity:

$$\frac{u_s - U_s}{U_*} = \frac{1}{\kappa}\left(1 + 2.3\log\frac{z}{h}\right)$$

or $$\frac{u_s}{U_s} = \frac{m+1}{m}\left(\frac{z}{h}\right)^{1/m}$$

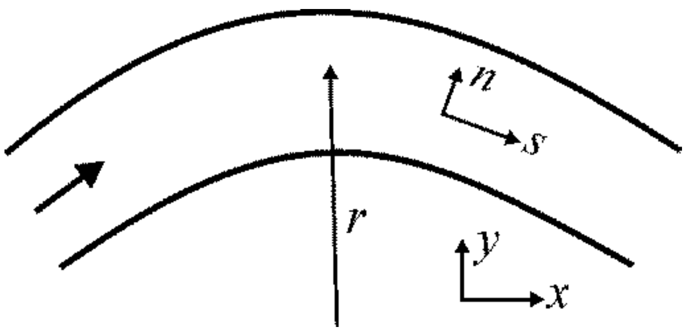

x- velocity:

$$u = \alpha_{11} u_s + \alpha_{12} u_n$$

$$= \alpha_{11}\frac{m+1}{m}U_s\left(\frac{z}{h}\right)^{1/m} + \alpha_{12}\left[U_n + b_s U_s \frac{h}{r}\left(2\frac{z}{h} - 1\right)\right]$$

Concentration distribution: $c = Cf(z)$

Integration of *x*- convection term:

$$\int_0^h ucdz = \alpha_{11}\frac{m+1}{m}U_s C\int_0^h\left(\frac{z}{h}\right)^{1/m} f(z)dz + \alpha_{12}U_n C\int_0^h f(z)dz$$

$$+\alpha_{12}b_s U_s C\frac{h}{r}\int_0^h\left(2\frac{z}{h}-1\right)f(z)dz$$

Using $\int_0^h f(z)dz = h,\quad \frac{m+1}{m}\int_0^h\left(\frac{z}{h}\right)^{1/m} f(z)dz \approx h$ leads to

$$D_{sx} = \frac{1}{h}\left(UhC - \int_0^h ucdz\right) = -\alpha_{12}b_s U_s C\frac{1}{r}\int_0^h\left(2\frac{z}{h}-1\right)f(z)dz$$

Similarly

$$D_{sy} = \frac{1}{h}\left(VhC - \int_0^h vcdz\right) = -\alpha_{22}b_s U_s C\frac{1}{r}\int_0^h\left(2\frac{z}{h}-1\right)f(z)dz$$

Dispersion of Momentum

$$D_{xx} = -\rho\left[\frac{1}{m(m+2)}\alpha_{11}\alpha_{11}U_s^2 + \frac{2b_s}{2m+1}\alpha_{11}\alpha_{12}IU_s + \frac{b_s^2}{3}\alpha_{12}\alpha_{12}I^2\right]$$

$$D_{xy} = -\rho\left[\frac{1}{m(m+2)}\alpha_{11}\alpha_{21}U_s^2 + \frac{b_s}{2m+1}(\alpha_{11}\alpha_{22} + \alpha_{12}\alpha_{21})IU_s + \frac{b_s^2}{3}\alpha_{12}\alpha_{22}I^2\right]$$

$$D_{yy} = -\rho\left[\frac{1}{m(m+2)}\alpha_{21}\alpha_{21}U_s^2 + \frac{2b_s}{2m+1}\alpha_{21}\alpha_{22}IU_s + \frac{b_s^2}{3}\alpha_{22}\alpha_{22}I^2\right]$$

Effects of Helical Flow

Clarkson UNIVERSITY defy convention

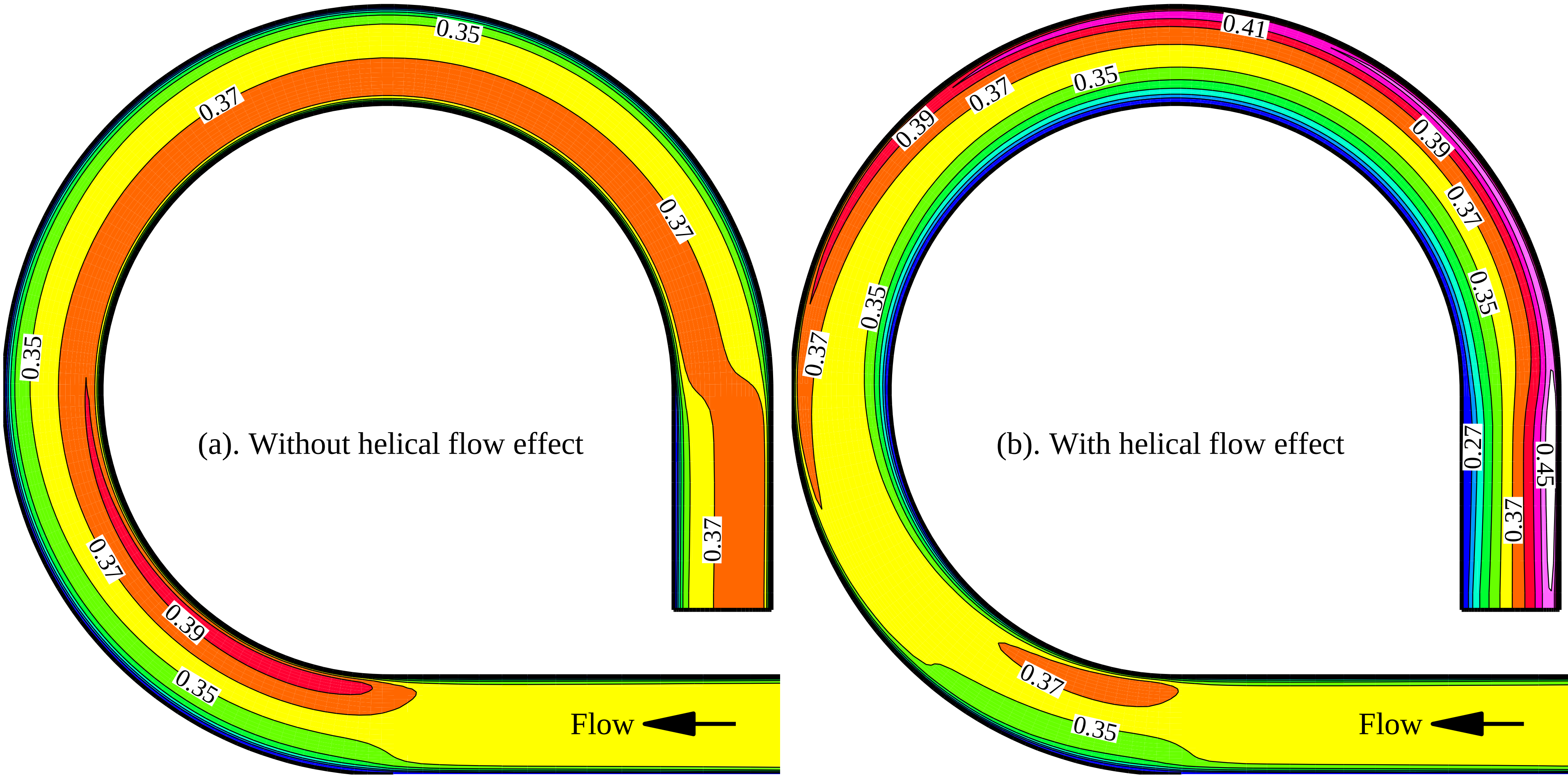

Calculated velocity contours without and with helical flow effect in Steffler's 270^{o} bend (Wu and Wang, 2004)

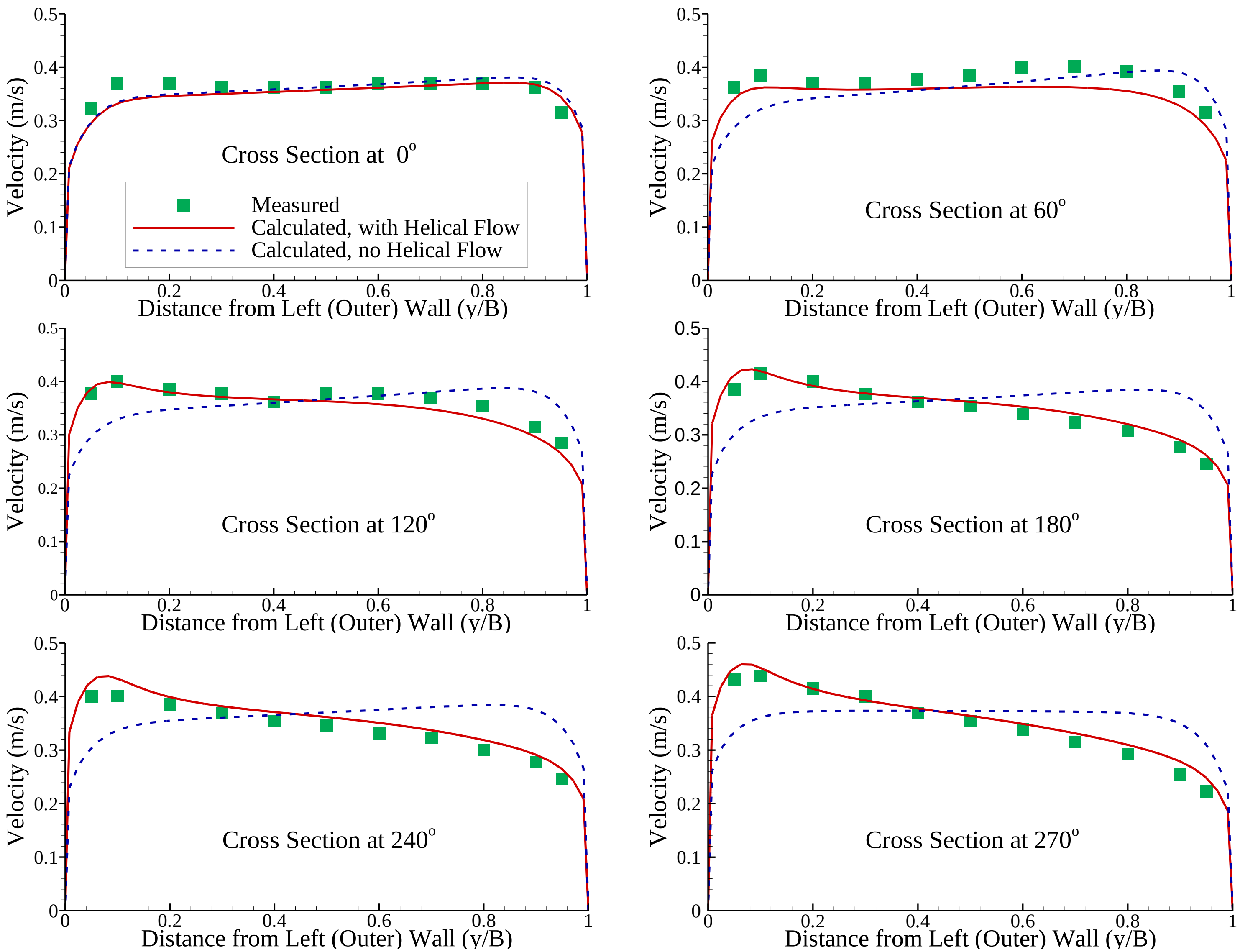

Measured vs. calculated velocities at selected cross-sections in Steffler's 270° bend (Calculations with and without helical flow effect, Wu and Wang, 2004)

FAST3D Simulation Results

FAST3D Model Validation in Channel Bend

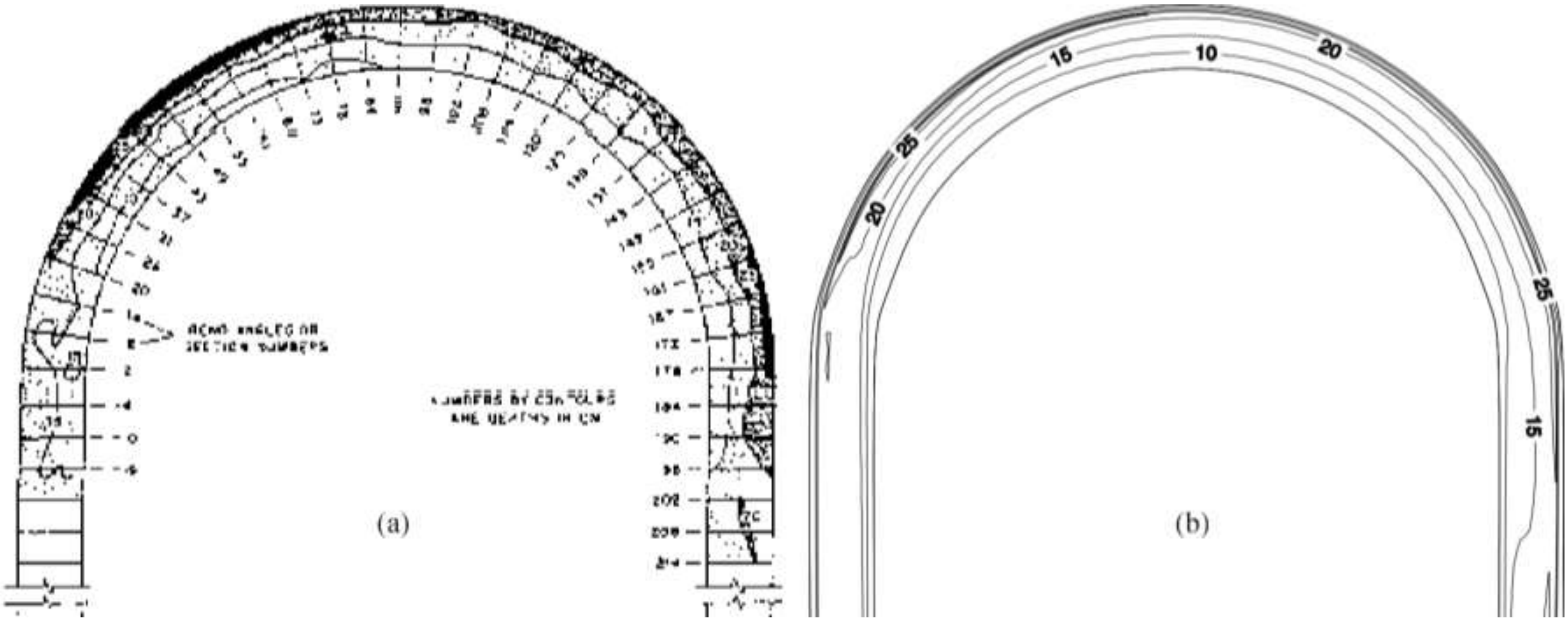

Flow depths: (a) Measured by Odgaard and Bergs (1988) and (b) Simulated by Wu et al. (2000)

FAST3D Simulation of Sedimentation Upstream of TGP Dam

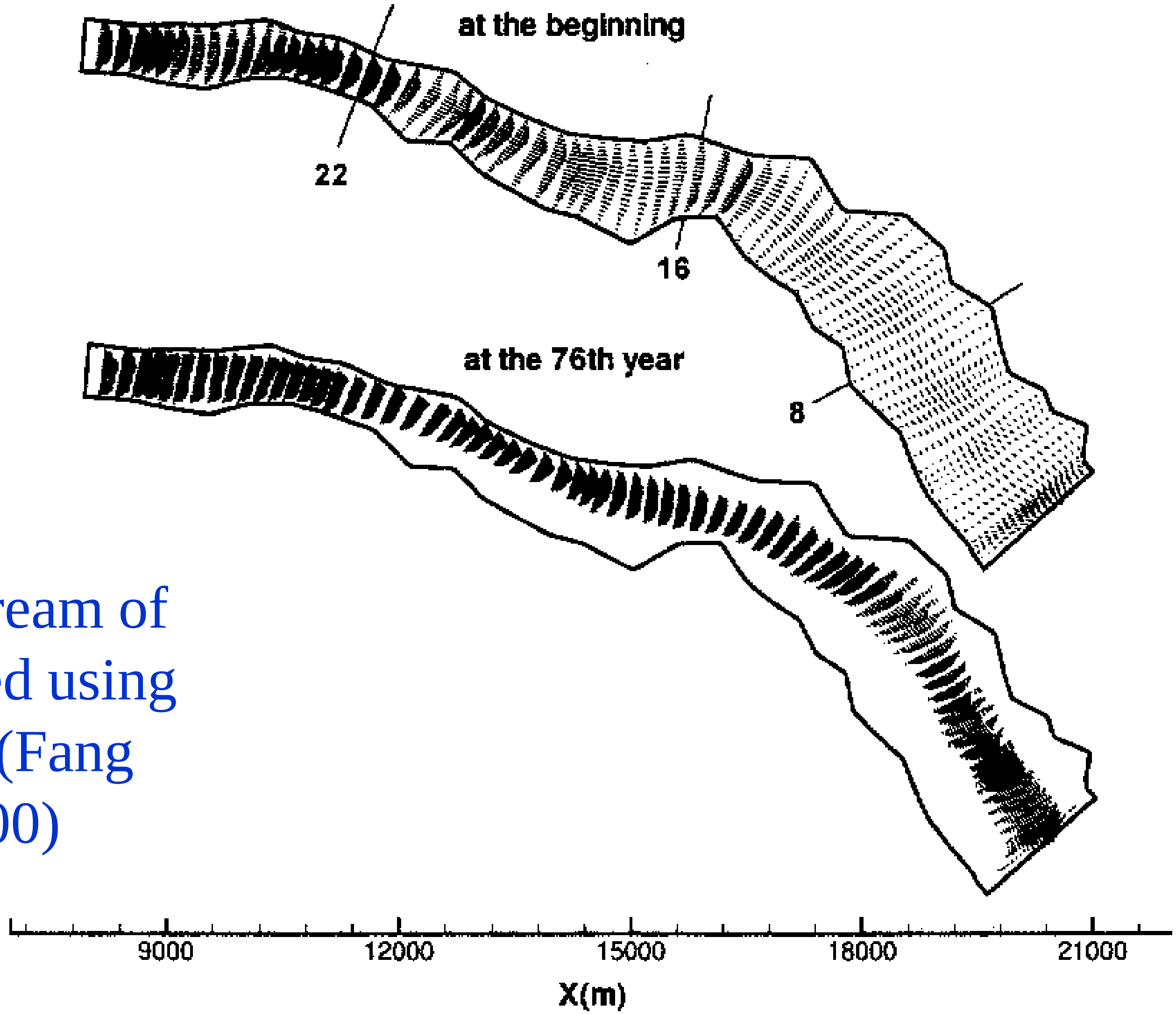

Flow pattern upstream of TGP dam simulated using FAST3D model (Fang and Rodi, 2000)

FAST3D Simulation of Sedimentation Upstream of TGP Dam

Flow velocity and bed surface at cross-sections (Fang and Rodi, 2000)

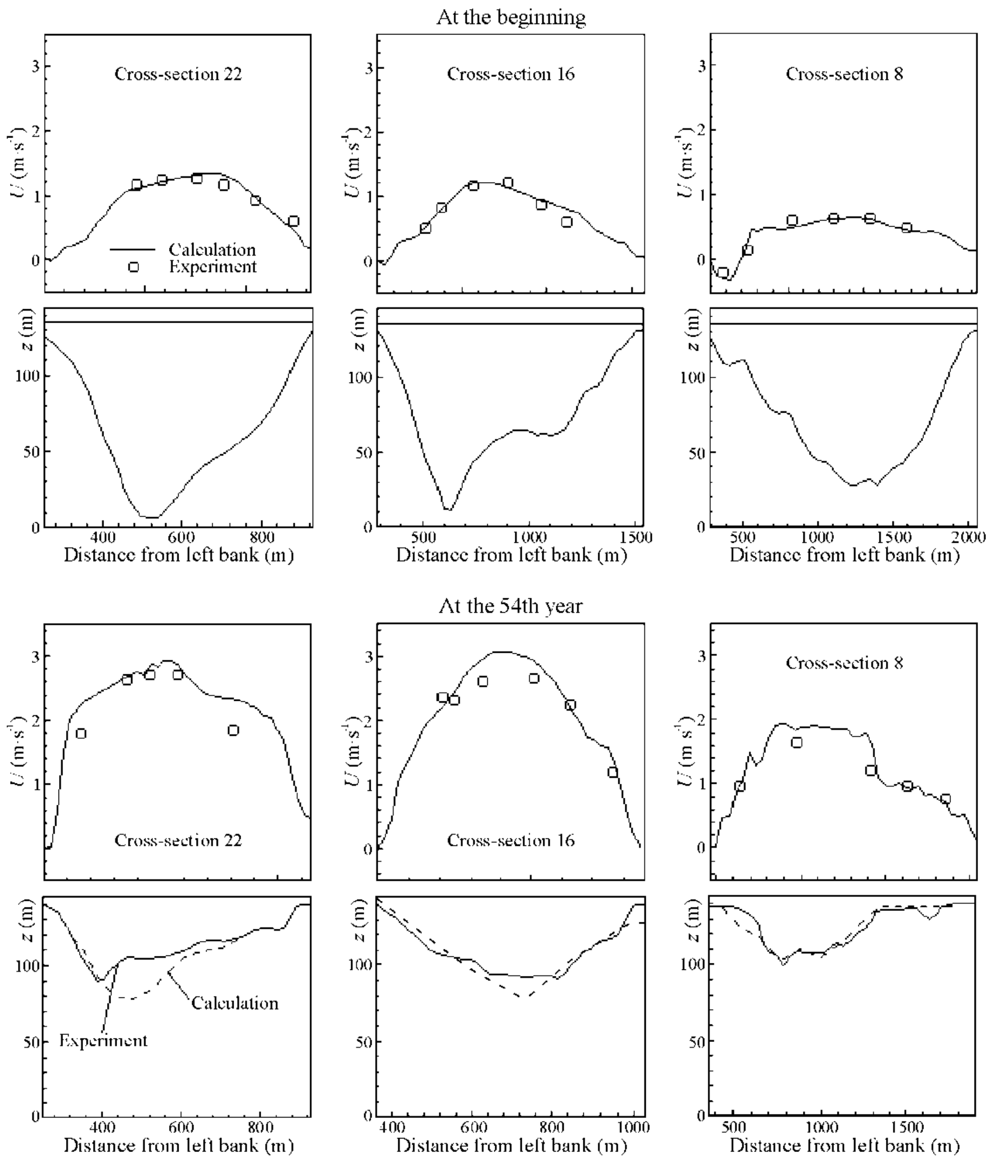

Local Scour near Instream Structures

Complexity of Flows near Structures

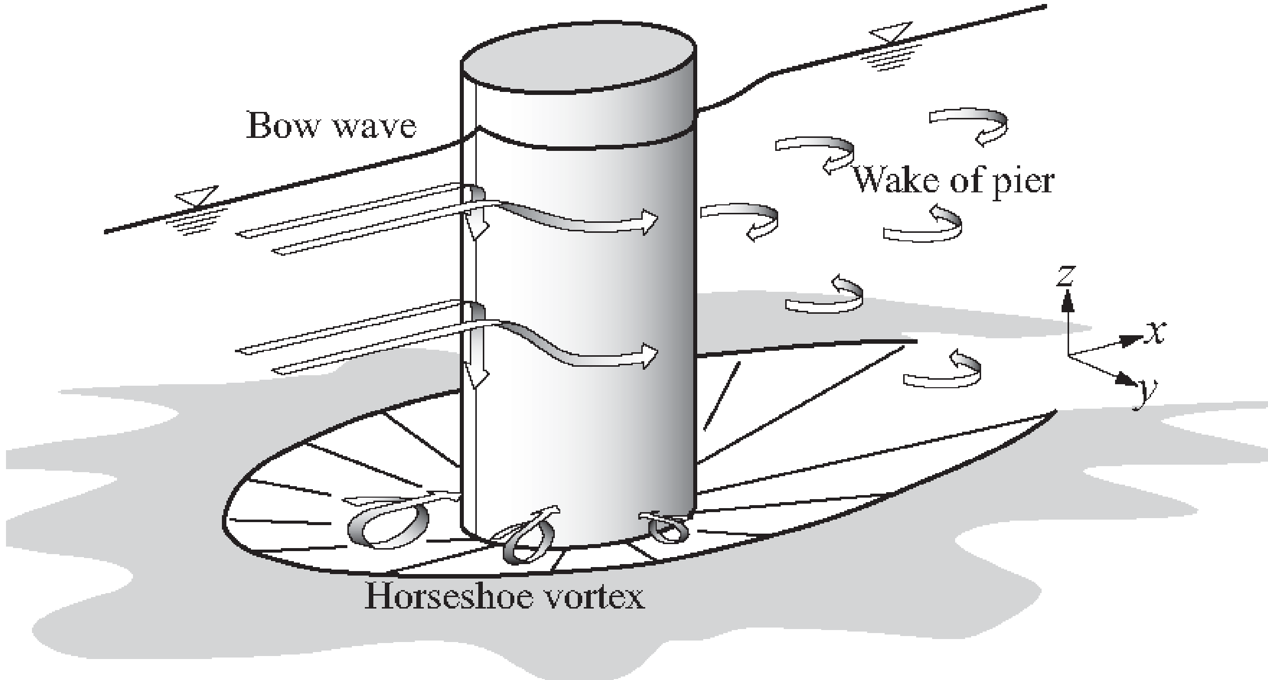

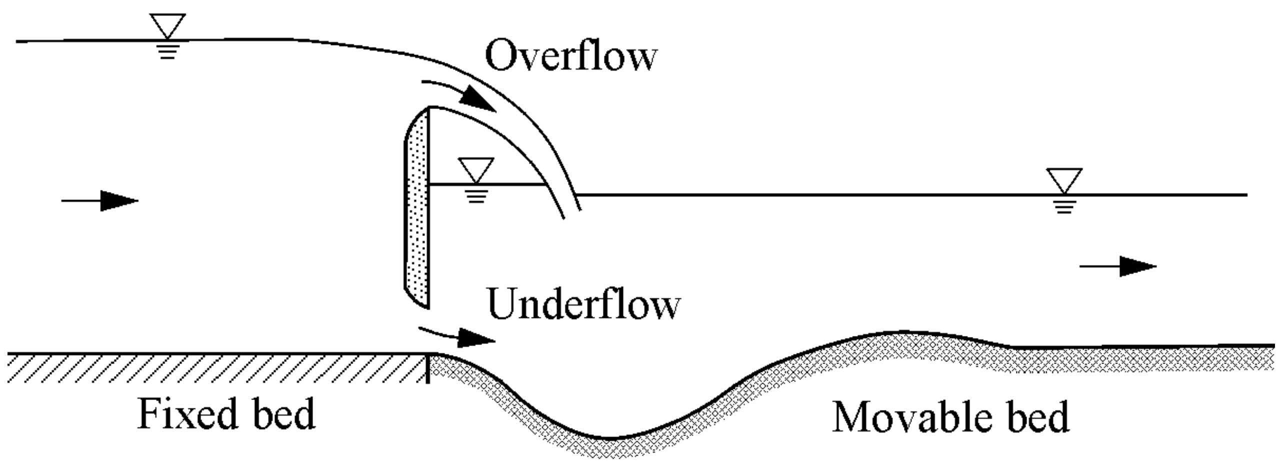

Significant Local Flow Features

- Localized dynamic pressure
- Horseshoe and other vortices
- Downward flow
- Turbulence intensified locally
- Pressure and shear stress fluctuations
- Flow unsteadiness
- Gravity effect on bed load
- Etc.

Forces on Sediment Particles

Generalized buoyancy force on a particle:

$$\vec{f}_p = -\frac{1}{6}\pi d^3 \nabla p$$

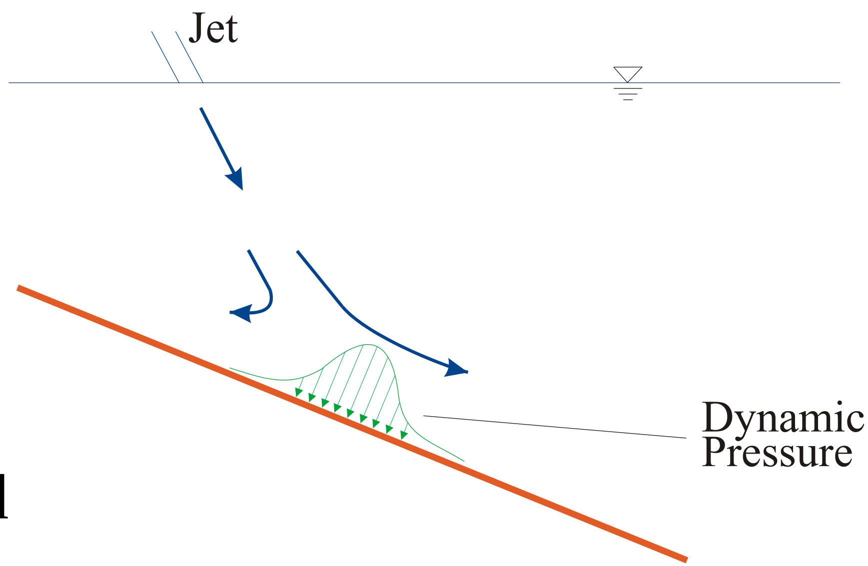

Effective tractive force per unit bed area in streamwise direction:

$$\tau_e = \tau_b' - \frac{a\pi}{6} d \left(\nabla p_d\right)_s$$

where p_d is dynamic pressure, d is sediment diameter, and a is coefficient assumed as 4/p.

Corrected Critical Shear Stress

$$\tau_c = K_p K_d K_s \tau_{c0}$$

Dynamic pressure gradient in vertical direction

$$K_p = 1 + \frac{1}{(\rho_s - \rho) g} \frac{\partial p_d}{\partial z}$$

Downward flow

$$K_d = 1/(1 + \sin\beta)$$

β is flow impact angle to the bed

Gravity over steep slope

$$K_s = \sin(\phi - \varphi)/\sin\phi$$

ϕ is repose angle and φ bed angle.

Sediment Transport Capacity

Modified Van Rijn's formulas

$$q_{b*} = 0.053\left(\frac{\rho_s - \rho}{\rho} g\right)^{0.5} \frac{d^{1.5}}{D_*^{0.3}}\left(\frac{\tau_e}{\tau_c} - 1\right)^{2.1}$$

$$c_{b*} = 0.015\frac{d}{bD_*^{0.3}}\left(\frac{\tau_e}{\tau_c} - 1\right)^{1.5}$$

Local Scour around a Bridge Pier

Scour depth contour at final time; simulation by FAST3D (Wu, 2007)

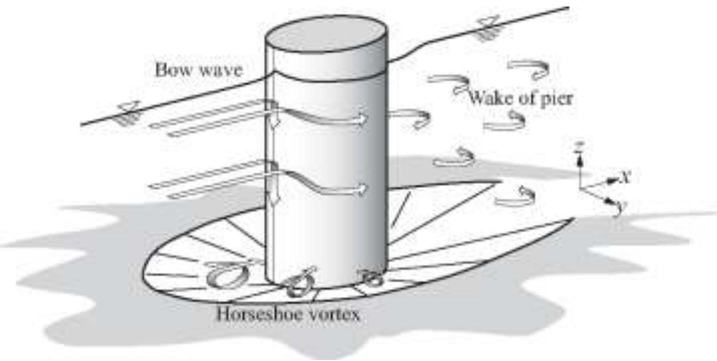

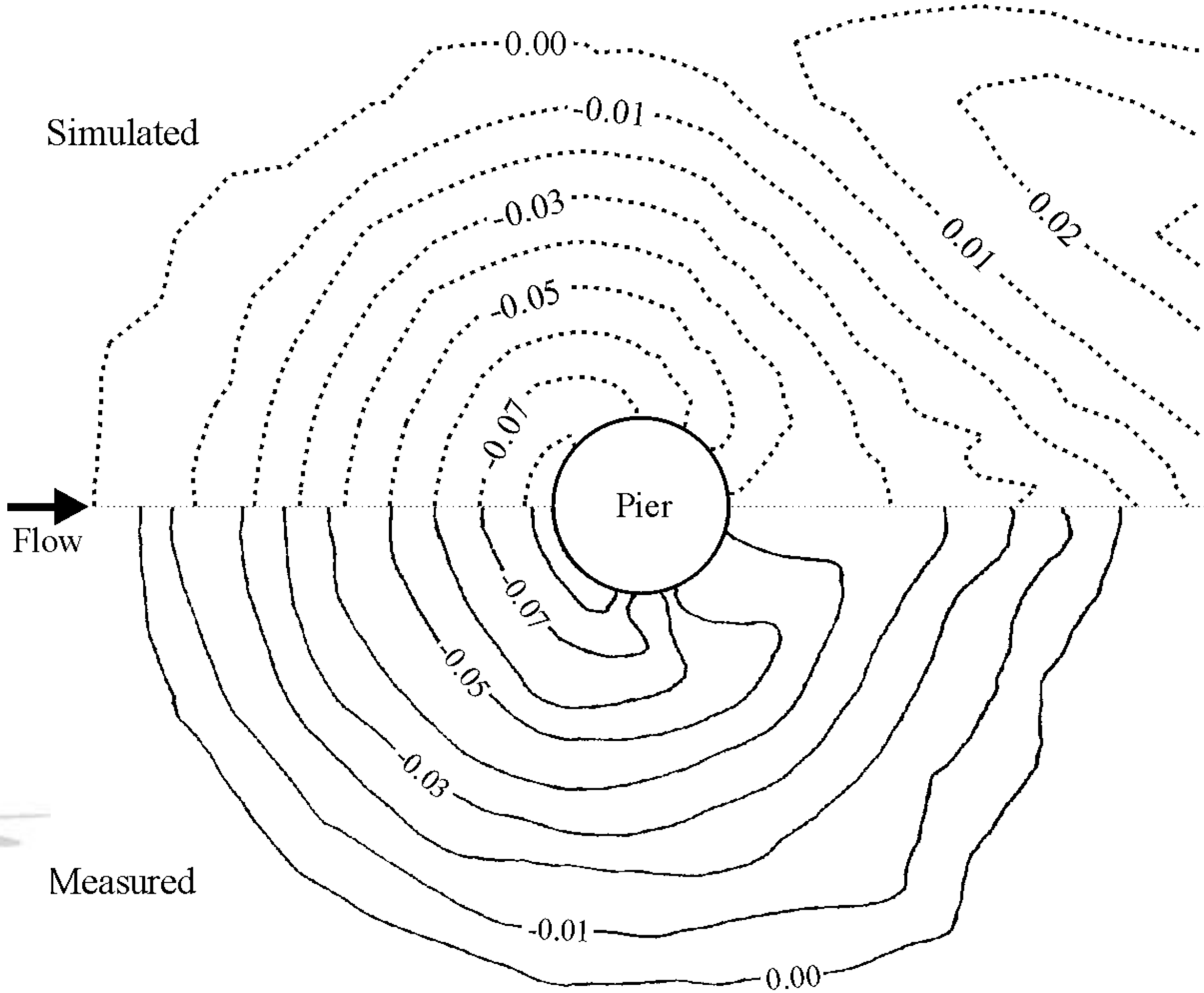

Local Scour around a Bridge Pier

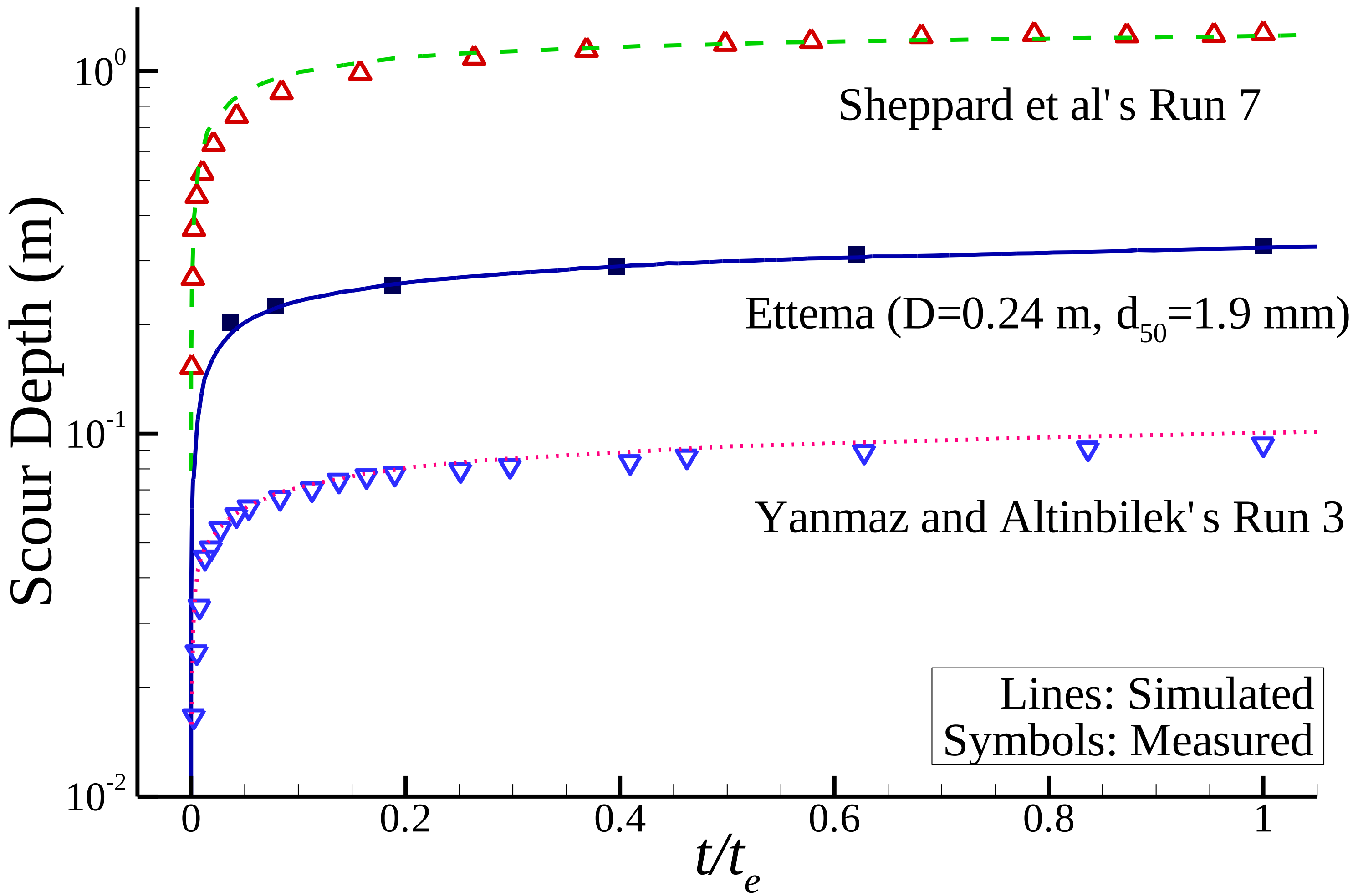

Scour depth with time (Wu, 2007)

Local Scour around a Bridge Pier

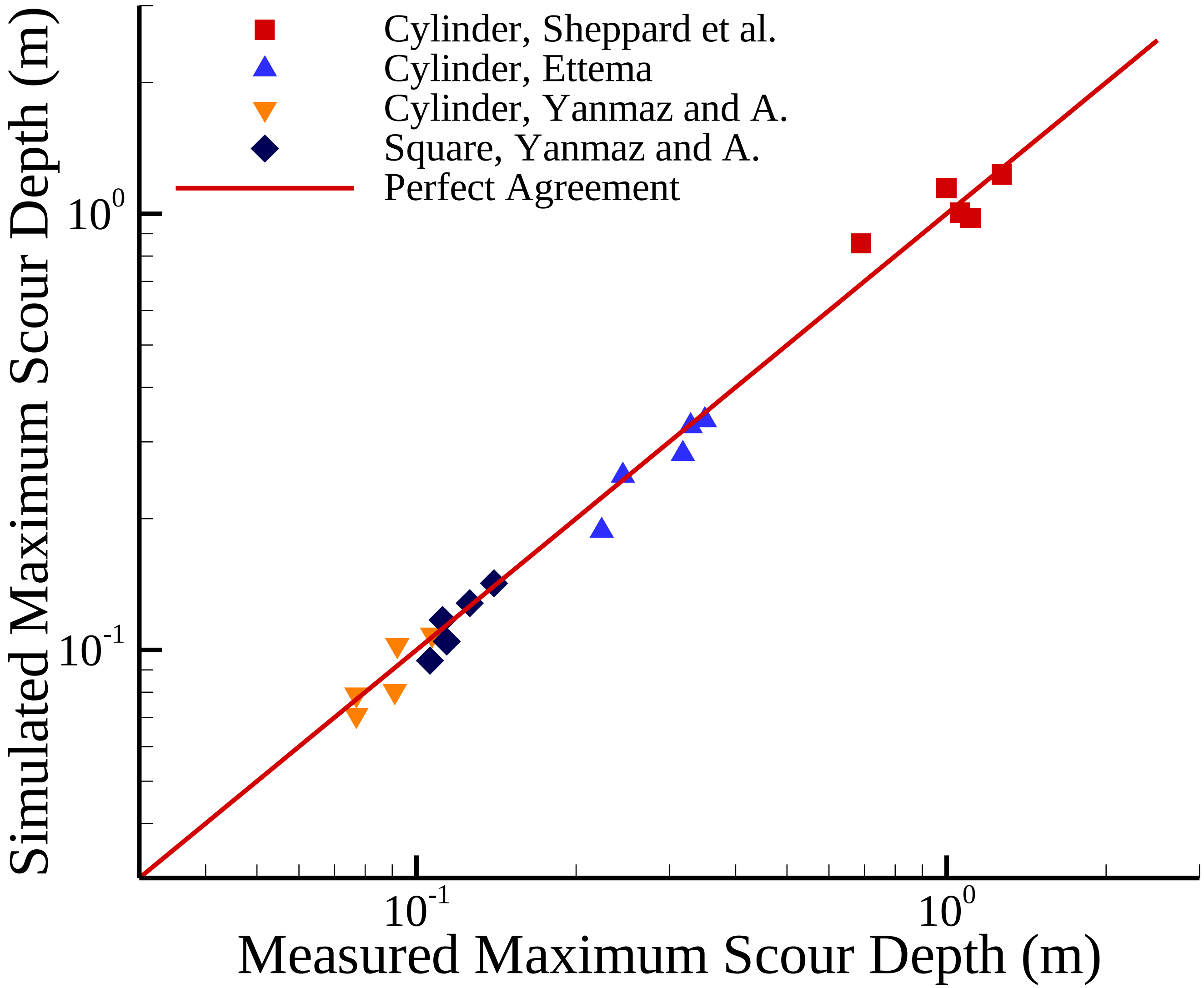

Headcut Migration

Headcut is an abrupt vertical or nearly vertical drop in stream bed, known as knickpoint. It may migrate upstream and cause significant soil erosion and channel instability..

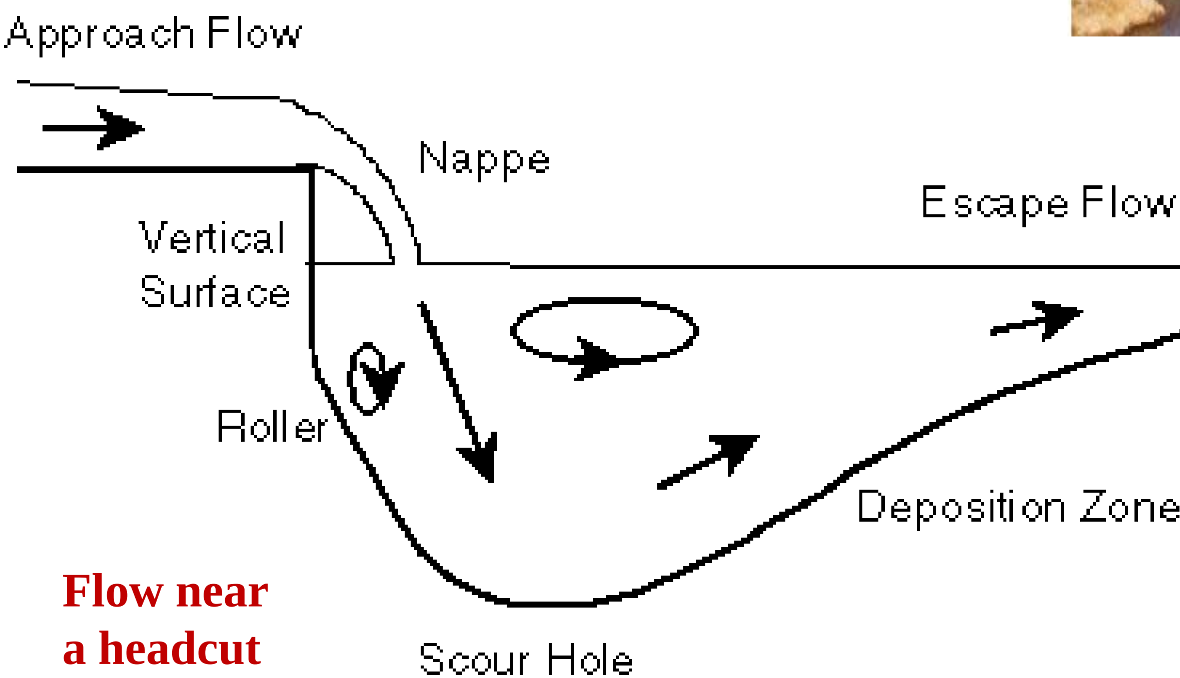

Flow near a headcut

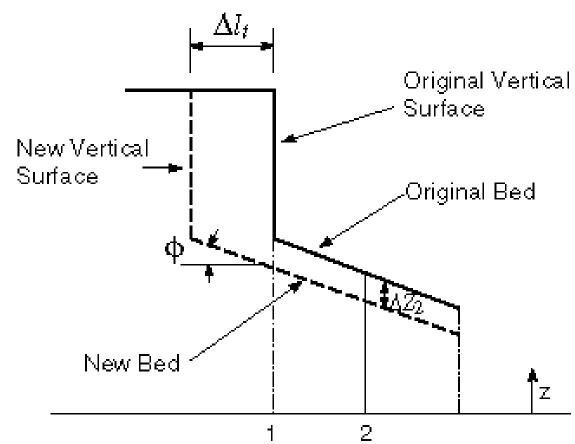

Headcut erosion model (Wu and Wang, 2005)

Headcut Migration

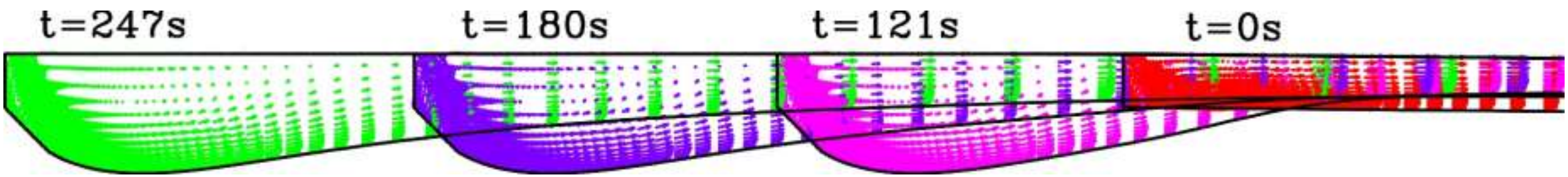

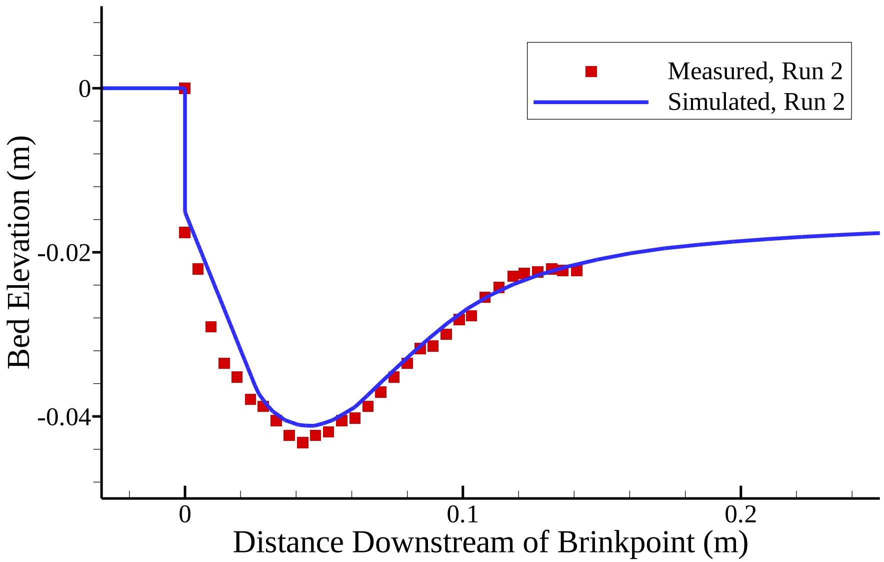

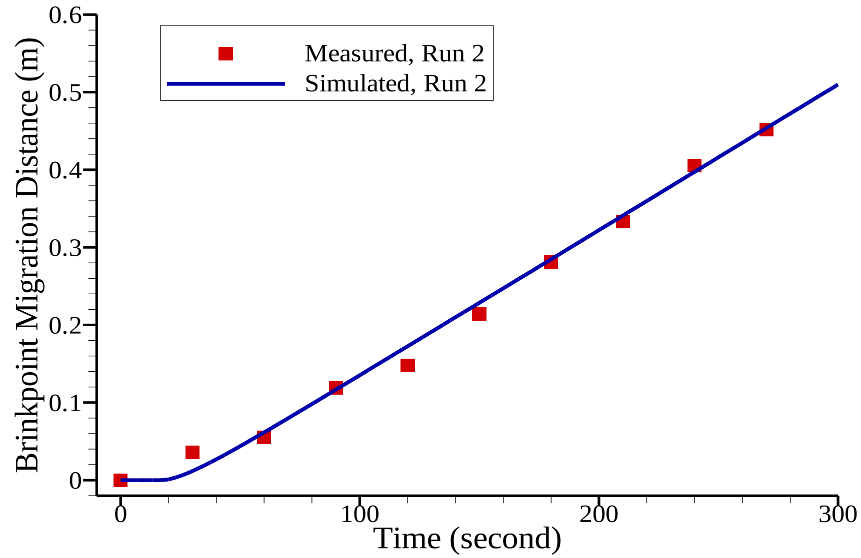

Simulation by Wu and Wang (2005)

Depth-Averaged 2-D Modeling of Local Scour (FASTER2D)

Depth-Averaged 2-D Formulation

Wu and Wang (ICSF-1, 2002):

$$\tau_e = \alpha_t \max\left(\tau_b, -\frac{\pi}{6} f d \rho g \frac{\partial z_s}{\partial s}\right)$$

with

$$f = \begin{cases} 3.4 D_*^{-0.3} f_s & D_* < 50 \\ 52.5 D_*^{-1} f_s & D_* \geq 50 \end{cases}$$

$$D_* = d\left[g(\rho_s/\rho - 1)/\nu^2\right]^{1/3}$$

$$\alpha_t = \left(\frac{\sigma}{\sigma_0}\right)\left[\int_0^\infty x^m e^{-0.5(x-p)^2} dx\right]^{1/m} \Bigg/ \left[\int_0^\infty x^m e^{-0.5(x-p_0)^2} dx\right]^{1/m}$$

2-D Model Used (FASTER2D)

- 2-D shallow water equations
- Standard k-ε turbulence model
- Finite volume method on curvilinear grid
- SIMPLEC algorithm on collocated grid, with Rhie and Chow's momentum interpolation
- Hybrid, QUICK, HLPA convection schemes
- SIP (Strongly Implicit Procedure)

2-D Simulation of Local Scour at Bridge Pier

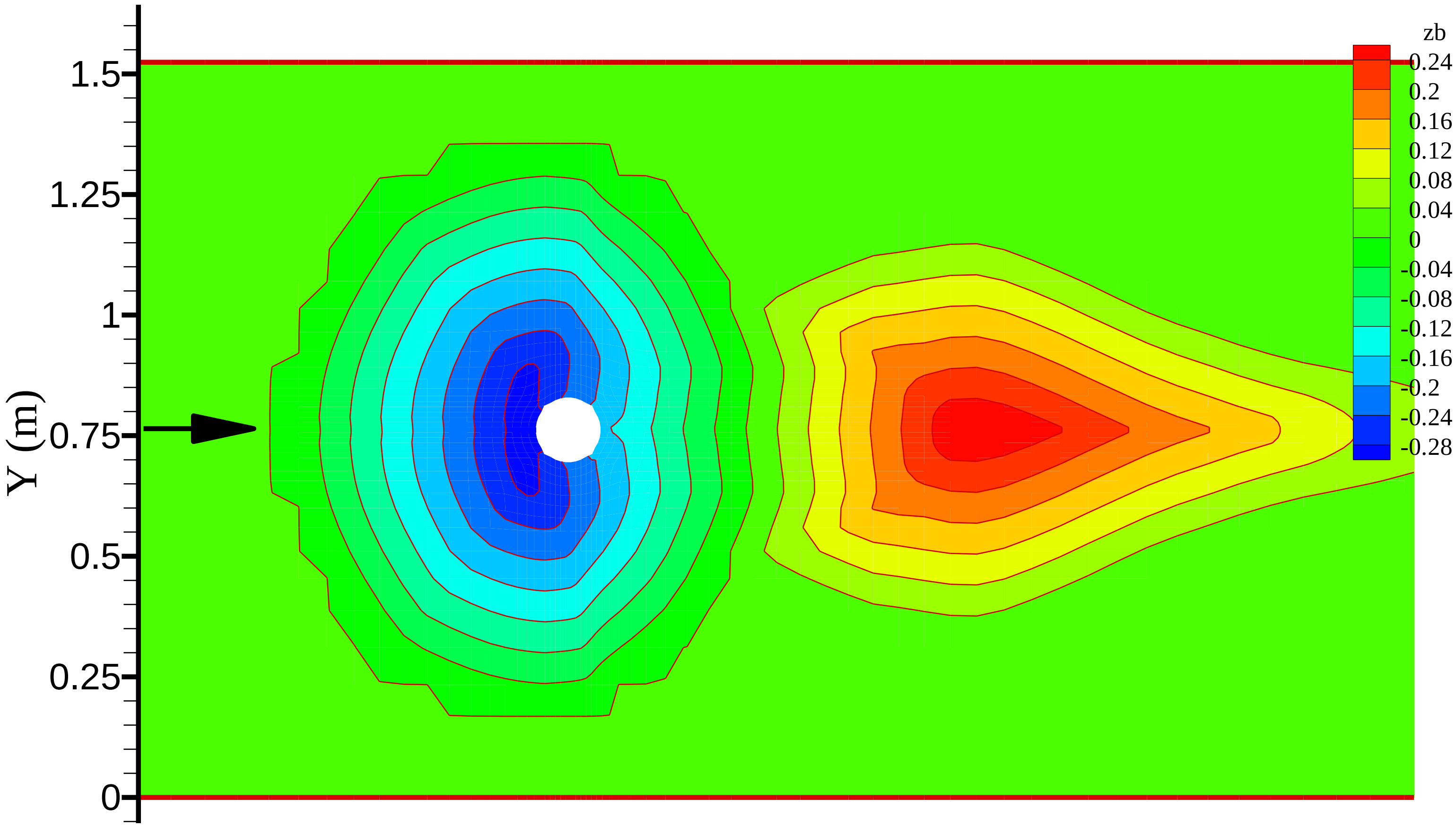

Note that the erosion pattern looks reasonable but the deposition not.

Validation of 2-D Model

34 cases in total:
6 spur-dikes,
3 square piers,
25 cylindrical
piers.

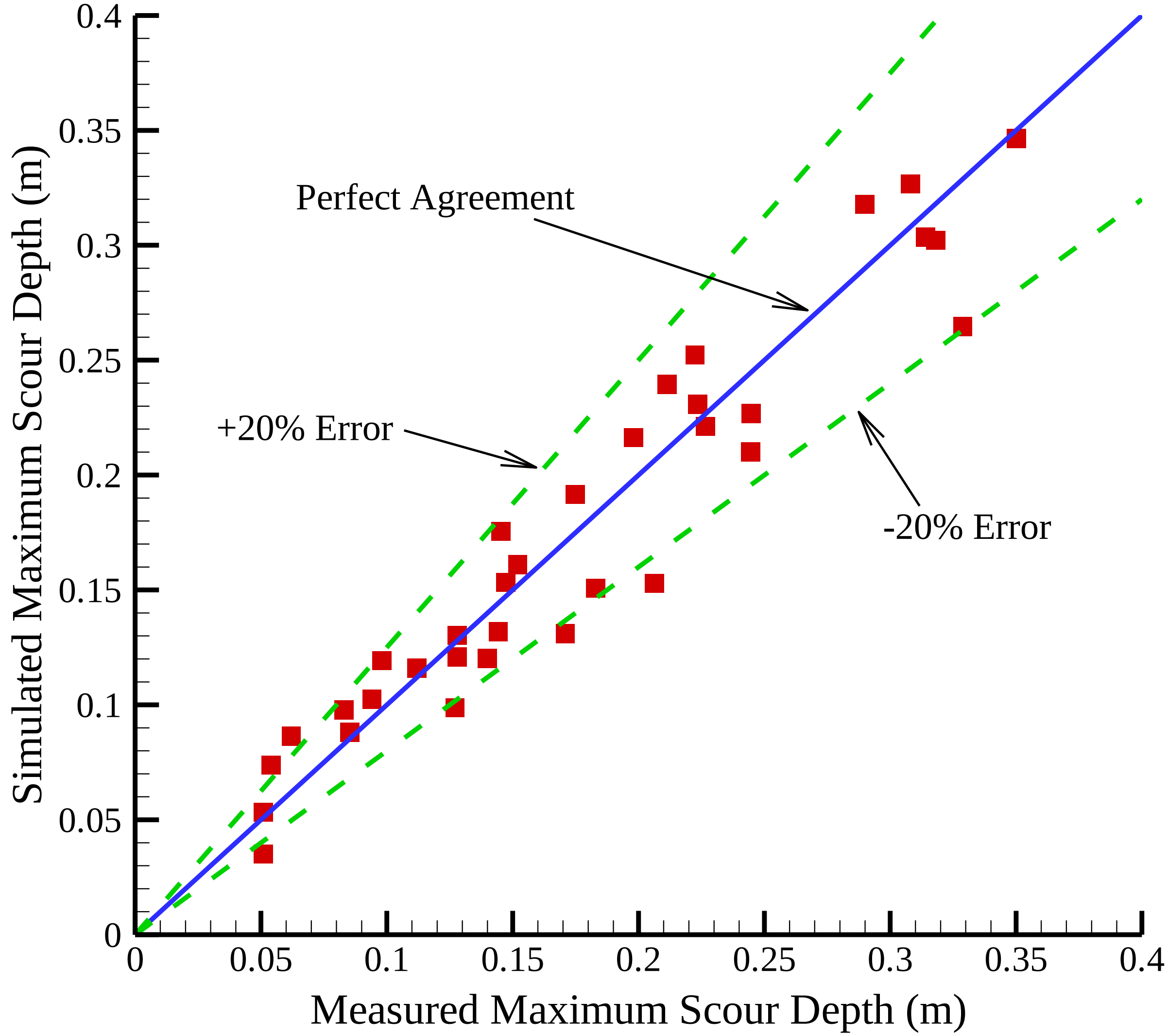

Local Scour Prediction Contest in ICSF-1

Experiment by Briaud et al., Texas A&M (2002)

Blind 2-D prediction using FASTER2D (Wu and Wang, 2002)

Case Description	Measured Max. Scour Depth	Calculated Max. Scour Depth
Case 1: 160 mm diameter circular pier placed in clean sand deposit of 0.3 mm in diameter and subjected to a constant velocity of 0.35 m/s and a depth of 0.375 m over a period of one day.	0.183 m	0.182 m
Case 2: 160 mm diameter circular pier placed in clean sand deposit of 0.3 mm and subjected to a multi-velocity hydrograph over a period of 4 days (25 m/s in day 1 and 0.35 m/s in day 2, and then each once in days 3 & 4).	0.185 m	0.205 m

Concluding Remarks

- 3-D flow features, such as localized dynamic pressure, downward flow, vorticity and turbulence, need to be considered in simulation of local scour near in-stream structures.
- A modification approach is proposed to extend the existing sediment entrainment functions to rapidly-varied (strongly non-uniform) flow conditions.
- The enhanced 3-D model predicts well the processes of bridge pier scour and headcut migration.
- The 2-D model with a simplified modification predicts reasonably well the maximum erosion depth, but errors exist in the deposition pattern behind the pier.
- The entrainment functions have not been directly validated by lab and field measurement data; all validations reported are indirect in conjunction with numerical models.

Publications Related

W. Wu, W. Rodi, and T. Wenka (2000). "3-D numerical modeling of water flow and sediment transport in open channels." J. Hydraulic Eng., ASCE, 126(1), 4–15.

W. Wu and S.S.Y. Wang (2002). "Prediction of local scour of non-cohesive sediment around bridge piers using FVM-based CCHE2D model," Proc. First International Conference on Scour of Foundations, Texas A&M University, Nov. 17-20. (on CD Rom)

W. Wu, D. A. Vieira, and S. S.Y. Wang (2004). "A 1-D numerical model for nonuniform sediment transport under unsteady flows in channel networks," J. Hydraulic Eng., ASCE, 130(9), 914–923.

W. Wu (2004). "Depth-averaged 2-D numerical modeling of unsteady flow and nonuniform sediment transport in open channels," J. Hydraulic Eng., ASCE, 130(10), 1013–1024.

W. Wu and S.S.Y. Wang (2004a). "Depth-averaged 2-D calculation of flow and sediment transport in curved channels," Int. J. Sediment Research, 19(4), 241–257.

W. Wu, P. Wang, and N. Chiba (2004). "Comparison of five depth-averaged 2-D turbulence models for river flows," Archives of Hydro-Engineering and Environmental Mechanics, Polish Academy of Science, 51(2), 183–200.

W. Wu, E. Jiang, and S. S.Y. Wang (2004). "Depth-averaged 2-D calculation of flow and sediment transport in the Lower Yellow River," Int. J. River Basin Management, IAHR, 2(1).

W. Wu and S. S.Y. Wang (2005). "Empirical-numerical analysis of headcut migration," Int. J. Sediment Research, 20(3), 233–243.

W. Wu, M. Altinakar, and S.S.Y. Wang (2006). "Depth-average analysis of hysteresis between flow and sediment transport under unsteady conditions," Int. J. Sediment Research, 21(2), 101–112.

W. Wu (2007), Computational River Dynamics, Taylor & Francis, UK, 494 p.